

## Temperature Dependence of the Electron Density of States and dc Electrical Resistivity of Disordered Binary Alloys\*

An-Ban Chen, Gideon Weisz, and Arden Sher†

*Department of Physics, College of William and Mary, Williamsburg, Virginia 23185*

(Received 27 September 1971)

A model calculation of the temperature dependence of the electronic density of states and the electrical conductivity of disordered binary alloys, based on the coherent-potential approximation (CPA) is made by introducing thermal disorder in the single-band model (Velický and others). Thermal disorder is found to broaden and smear the static-alloy density of states. The electrical resistivity in weak-scattering alloys always increases with temperature. However, in the strong-scattering case, the temperature coefficient of resistivity can be positive, zero, or negative, depending on the location of the Fermi energy.

### I. INTRODUCTION

The macroscopic electronic properties of alloys,<sup>1</sup> such as the dc electrical resistivity, have been fruitful subjects for experiments,<sup>2</sup> because useful devices, e.g., strain gauges, have been constructed which depend on these properties, they can be measured accurately, and the results of these experiments provide an insight into the microscopic behavior of the materials. The theoretical interpretation of these properties has lagged far behind the wealth of experimental information. For example, it is well known that constantan has a very constant resistivity over a wide range of temperature,<sup>2</sup> a fact not explained by the standard theory. A more striking example is Fe<sub>70</sub>Cr<sub>20</sub>Al<sub>10</sub> alloy,<sup>3</sup> which has a substantial decrease in electrical resistivity as temperature increases from 77 to 1200 °K. Because of a formidable combination of complexities (a discussion of this point is given in Sec. V F), a genuine understanding of these facts remains a challenging theoretical problem. It is too early a stage in the development of alloy theory to give a first-principles quantitative description of the transport properties of concentrated strong-scattering disordered systems, like constantan, since the easier and more basic electronic quantity, the static-alloy density of states, is just beginning to be understood.<sup>4-7</sup> At present, even a qualitative or model description of the transport properties in such alloys is greatly needed. The object of this work is to understand the temperature variation of the alloy density of states and conductivity which results from the interplay between the alloy disorder and thermal disorder.

The paper is outlined as follows. We start by introducing the formal theory in Sec. II where the density of states and the conductivity are related to the averaged Green functions. Then a general discussion of the temperature-dependent aspects

of the formulas is given along with a review of related works (Sec. III). After giving a summary of the formalism of the coherent-potential approximation<sup>4,8,9</sup> (CPA) (Sec. IV), we present a model calculation based on CPA (Sec. V).

In the model calculation, we use a model Hamiltonian similar to that of Velický *et al.*,<sup>4</sup> but with thermal disorder added. A new interpretation of the basis and matrix elements which enter into the formalism is given, and this is then incorporated in the matrix manipulation of the averaged Green function. The thermal-disorder Hamiltonian takes the usual form containing one-phonon creation and annihilation operators. Working within this model, we reduce the CPA self-consistent operator equation to a scalar integral equation for the self-energy. In order to obtain the numerical results, we use simple forms for the input functions: a semiellipse for the pure crystal density of states, a velocity-functional form proportional to the density of states, and a Gaussian distribution governing the thermal fluctuation of the random atomic energy levels. Following a detailed discussion of the numerical method of solving the integral equation, we present the results of numerical computations for some representative parameters. A systematic study of self-energies, the total density of states, the component density of states, and the conductivity is exhibited in the form of three-dimensional plots. Thermal disorder is found to smear and broaden the static-alloy density of states. Disorder always increases the electrical resistivity in the weak-scattering limit. However, in the strong-scattering case, the conductivity may decrease, increase, or remain constant with temperature depending on the location of the Fermi energy.

The numerical results are followed by a discussion of the implications of the model calculation. The nonperturbation nature of the problem is briefly mentioned; then an interpretation of the self-energy

in the averaged Green function is given. We show that the relaxation time, corresponding to the imaginary part of the self-energy appearing in the formulas for the density of states and the conductivity, is not the usual decay time of the Bloch states, but rather is the decay time for a different process. However, in the weak-scattering limit, there is no distinction between these two relaxation times. We also, by a proper choice of the relaxation time and the Fermi velocity, reduce the CPA conductivity formula to the customary form in the weak-scattering limit, which aids in the physical interpretation of the results. In the strong-scattering case, and in instances where the conductivity increases with temperature, we interpret the results as approaching the regime where the thermal fluctuations assist the motion of highly damped "quasilocalized" electrons.

Finally, an analysis of the problems associated with a real transition-metal alloy is given. From this, we can see how far we are from the goal of a quantitative theory of transition-metal alloys.

## II. DENSITY OF STATES, CONDUCTIVITY, AND THE GREEN FUNCTION IN A DISORDERED SYSTEM

Transport properties, such as electrical conductivity, are often obtained from solutions to the Boltzmann equation. But the semiclassical Boltzmann equation is not valid if the uncertainty in the momentum of the carrier is greater than the momentum itself. This is equivalent to the Landau-Peierls<sup>10</sup> criterion for the validity of Boltzmann equation:

$$\mathcal{E}_F \tau \geq \hbar \quad (1)$$

To avoid this difficulty, we have to use a quantum-mechanical approach to the transport properties. One approach is to use some quantum transport equation, such as Van Hove's<sup>11</sup> generalized master equation, but the application of this method is not well developed in the literature, since his integral equation is too difficult to solve. Other, more manageable transport equations, such as the Kohn-Luttinger type,<sup>12,13</sup> are perturbation theoretic, and depend on the existence of a small parameter, such as a small impurity concentration or weak scattering; therefore, we cannot use such a method for a concentrated strong-scattering alloy. Another, more popular approach will be used here, namely, the density-matrix method of the Kubo linear-response theory,<sup>14,15</sup> which is both rigorous and convenient. A good comparison of the Kubo and Kohn-Luttinger methods is given by Moore.<sup>16</sup> Our starting point, the Kubo formula for the electrical conductivity, is obtained from a formal solution to the Liouville equation of the density matrix to first order in the external electrical field. The

formal expression for the dc electrical conductivity tensor  $\sigma^{\alpha\beta}$  is<sup>14</sup>

$$\sigma^{\alpha\beta} = (1/\Omega) \int_0^\infty dt \int_0^{1/\kappa T} d\lambda \langle J_\beta(-i\hbar\lambda) J_\alpha(t) \rangle, \quad (2)$$

where  $J_\alpha(t)$  is the  $\alpha$  component of the total-current operator in the unperturbed Heisenberg picture,

$$J_\alpha(t) = e^{i\mathcal{H}t/\hbar} J_\alpha e^{-i\mathcal{H}t/\hbar}, \quad (3)$$

and  $\Omega$  is the volume of the system,  $\kappa$  is Boltzmann's constant, and  $T$  is the temperature. In Eq. (3),  $\mathcal{H}$  is the total Hamiltonian of the system before the field is turned on. The brackets  $\langle \rangle$  in Eq. (2) mean the ensemble average, i. e.,

$$\langle A \rangle = \text{Tr}[\rho_e(\mathcal{H})A], \quad (4)$$

where  $\rho_e(\mathcal{H})$  is the equilibrium density matrix. The Hamiltonian generally includes all the subsystem Hamiltonians, e. g., electrons, phonons, spin waves, etc., and the interactions among them. We shall restrict ourselves to an alloy composed of  $N$  atoms and  $cN$  electrons. The appropriate Hamiltonian of the alloy is

$$\mathcal{H} = \sum_i H(\vec{r}_i; \vec{R}_1, \vec{R}_2, \dots, \vec{R}_N) + H_{\text{ion}}(\vec{R}_1, \dots, \vec{R}_N), \quad (5)$$

where the one-electron Hamiltonian  $H$  takes the form

$$H(\vec{r}) = p^2/2m + V(\vec{r}; \vec{R}_1, \vec{R}_2, \dots, \vec{R}_N), \quad (6)$$

where  $V(\vec{r}; \vec{R}_1, \vec{R}_2, \dots, \vec{R}_N)$  is the appropriate screened-ionic potential when the ions are located at positions  $\vec{R}_1$  through  $\vec{R}_N$ . Notice that  $H$  depends on the locations of the ions. The eigenfunctions of  $H$  and eigenvalues are defined by

$$H(\vec{r}; \vec{R}_1, \dots, \vec{R}_N) \Psi_a(\vec{r}; \vec{R}_1, \dots, \vec{R}_N) = \mathcal{E}_a \Psi_a(\vec{r}; \vec{R}_1, \dots, \vec{R}_N). \quad (7)$$

In a static alloy the positions of the ions are fixed so  $H$  commutes with  $H_{\text{ion}}$ , and the Kubo formula, Eq. (2), can be reduced<sup>17</sup> to the Greenwood formula<sup>18</sup>

$$\sigma^{\alpha\beta} = \frac{2\pi e^2 \hbar}{\Omega} \left\langle \sum_a \sum_b \left( -\frac{\partial f}{\partial \mathcal{E}_a} \right) \delta(\mathcal{E}_a - \mathcal{E}_b) v_{ab}^\alpha v_{ba}^\beta \right\rangle_c, \quad (8)$$

where  $a$  and  $b$  are quantum numbers defined in Eq. (7), and  $v_{ab}^\alpha$  is the electron velocity matrix element

$$v_{ab}^\alpha = (1/m) \langle \Psi_a | p^\alpha | \Psi_b \rangle, \quad (9)$$

where  $p^\alpha$  is the  $\alpha$  component of the electron-momentum operator. In Eq. (8),  $\langle \rangle_c$  means an average over all the substitutional arrangements of the ions, usually called the "configuration average." The function  $f$  in Eq. (8) is the Fermi-Dirac distribution

$$f(\mathcal{E}) = 1/(e^{\beta(\mathcal{E}-\mu)} + 1), \quad (10)$$

where  $\beta = (\kappa T)^{-1}$  as usual, and  $\mu$  is the chemical potential energy.

In general, the one-electron Hamiltonian  $H$  does not commute with the ionic Hamiltonian  $H_{\text{ion}}$ . It is a rather difficult problem trying to carry out the trace by any kind of perturbation expansion in Eq. (2). However, we can approximate in the spirit of the Born-Oppenheimer adiabatic approximation at this point. Since the ionic motion is slow compared to the electron motion, i. e.,  $v_{\text{ion}}/v_{\text{elec}} \sim 10^{-3}$ , we can freeze the ionic positions and solve for electronic states, i. e., Eq. (7). Then we can find the expectation value of the electronic quantities in this particular ionic configuration. Finally, we can average the expectation value over all possible positions of the ions in the given configuration, and then over all possible configurations to get the macroscopic expectation value. Applying this to the electrical resistivity, the Kubo-Greenwood formula [Eq. (8)] is merely modified by an extra average,

$$\sigma^{\alpha\beta} = \frac{2\pi e^2 \hbar}{\Omega} \left\langle \left\langle \sum_a \sum_b \left( -\frac{\partial f}{\partial \mathcal{E}_a} \right) \delta(\mathcal{E}_a - \mathcal{E}_b) v_{ab}^\alpha v_{ba}^\beta \right\rangle_b \right\rangle_c, \quad (11)$$

where  $\langle \rangle_b$  means an average over the ionic positions. We shall drop the indices from the double average in what follows.

When Eq. (11) is applied to a liquid metal, we do not need the configuration average  $\langle \rangle_c$ . Then Eq. (11) is identical with the equation used by Edwards.<sup>19</sup> To be explicit, let us define the alloy electronic spectral density matrices  $\rho_1$ ,  $\rho_2$ , etc., following Edwards:

$$\begin{aligned} \rho_1(\vec{r}_1, \vec{r}'_1; E) &= \langle \int [\sum_a \Psi_a^*(\vec{r}_1; \vec{R}_1, \dots, \vec{R}_N) \Psi_a(\vec{r}'_1; \vec{R}_1, \dots, \vec{R}_N) \\ &\quad \times \delta(\mathcal{E}_a - E)] P_c(\vec{R}_1, \dots, \vec{R}_N) \prod_i d^3 R_i \rangle_c \\ &= \langle \langle \sum_a \Psi_a^*(\vec{r}_1) \Psi_a(\vec{r}'_1) \delta(E - \mathcal{E}_a) \rangle \rangle, \quad (12) \end{aligned}$$

and

$$\begin{aligned} \rho_2(\vec{r}_1, \vec{r}'_1; \vec{r}_2, \vec{r}'_2; E_1, E_2) &= \langle \langle \sum_a \sum_b \Psi_a^*(\vec{r}_1) \Psi_a(\vec{r}'_1) \Psi_b^*(\vec{r}_2) \Psi_b(\vec{r}'_2) \\ &\quad \times \delta(E_1 - \mathcal{E}_a) \delta(E_2 - \mathcal{E}_b) \rangle \rangle, \quad (13) \end{aligned}$$

where  $P_c(\vec{R}_1, \dots, \vec{R}_N)$  is the distribution function of ionic positions  $(\vec{R}_1, \dots, \vec{R}_N)$  in a particular ionic configuration, as indicated by the index  $c$ . Explicitly,  $P_c$  is

$$P_c = \sum_\gamma |\Phi_\gamma^c(\vec{R}_1, \dots, \vec{R}_N)|^2 e^{-\beta E_\gamma^c} (\sum_{c', \gamma'} e^{-\beta E_{\gamma'}^{c'}})^{-1}, \quad (14)$$

where  $\Phi_\gamma^c$  is the eigenfunction of  $H_{\text{ion}}$  with the eigenvalue  $E_\gamma^c$  in a particular configuration  $c$ , so that

$$H_{\text{ion}}(\vec{R}_1, \dots, \vec{R}_N) \Phi_\gamma^c(\vec{R}_1, \dots, \vec{R}_N) = E_\gamma^c \Phi_\gamma^c(\vec{R}_1, \dots, \vec{R}_N). \quad (15)$$

Equations (12) and (13) serve to define the double average explicitly. They are also useful to connect the quantities of interest to us, i. e., density of states and electrical conductivity, to the Green function, as follows.

The electronic density of states per atom is

$$\mathfrak{N}(E) = (1/N) \int d^3 r \rho_1(\vec{r}, \vec{r}; E). \quad (16)$$

The electrical conductivity is related to  $\rho_2$  by

$$\begin{aligned} \sigma^{\alpha\beta} &= \frac{2\pi e^2 \hbar^3}{m^2 \Omega} \int d\eta \left( -\frac{df}{d\eta} \right) \int d^3 r_1 d^3 r_2 \\ &\quad \times \nabla_1'^\alpha \nabla_2'^\beta \rho_2(\vec{r}_1, \vec{r}'_1; \vec{r}_2, \vec{r}'_2; \eta, \eta) \Big|_{\vec{r}_1=\vec{r}'_1, \vec{r}_2=\vec{r}'_2}. \quad (17) \end{aligned}$$

Let us define a Green function of complex argument  $z$  associated with  $H$ ,

$$G(z) = [z - H]^{-1} = \sum_a \frac{|\Psi_a\rangle \langle \Psi_a|}{z - \mathcal{E}_a}, \quad (18)$$

which is analytic everywhere except for a line of poles  $\{\mathcal{E}_a\}$ , which for large  $\Omega$  is equivalent to a branch cut along the real axis, where the spectrum of  $H$  lies.

Using the identity<sup>20</sup>

$$\frac{1}{x \pm i0} = \mathcal{P} \frac{1}{x} \mp i\pi \delta(x), \quad (19)$$

we can easily show that Eq. (16) is equivalent to

$$\mathfrak{N}(E) = \pm (1/N\pi) \text{Im Tr} \langle \langle G(E \mp i0) \rangle \rangle,$$

We can also rewrite Eq. (11) or Eq. (17) in the operator form

$$\sigma^{\alpha\beta} = \frac{2\pi e^2 \hbar}{m^2 \Omega} \int d\eta \left( -\frac{df}{d\eta} \right) \text{Tr} \langle \langle p^\alpha \delta(\eta - H) p^\beta \delta(\eta - H) \rangle \rangle, \quad (21)$$

or, when the delta functions are expressed in terms of the Green function through Eqs. (18) and (19),  $\sigma^{\alpha\beta}$  becomes

$$\sigma^{\alpha\beta} = \frac{2\pi e^2 \hbar}{m^2 \Omega} \int d\eta \left( -\frac{df}{d\eta} \right) I_{p^\alpha p^\beta}(\eta, \eta), \quad (22)$$

where

$$\begin{aligned} I_{p^\alpha p^\beta}(\eta, \eta) &= (1/4\pi^2) \text{Tr} \{ p^\beta [K(\eta^+, p^\alpha, \eta^-) + K(\eta^-, p^\alpha, \eta^+) \\ &\quad - K(\eta^+, p^\alpha, \eta^*) - K(\eta^-, p^\alpha, \eta^*)] \}, \quad (23) \end{aligned}$$

with

$$K(z_1, p^\alpha, z_2) = \langle \langle G(z_1) p^\alpha G(z_2) \rangle \rangle. \quad (24)$$

In Eq. (23),  $\eta^*$  means  $\eta \pm i0$ .

So far, the formulas, Eqs. (20) and (22), are still very general; they can apply to any disordered system. Thus, to solve for the density of states, we need to average the one-electron Green function  $G$ ; while for conductivity, we need, loosely speak-

ing, an average of the product of two Green functions  $\langle\langle GG \rangle\rangle$ .

However, the conductivity formula, Eq. (22), is only an approximation to the exact Kubo formula, Eq. (2). It is valid whenever the ionic motion can be treated classically, or, equivalently, when we can neglect the noncommutation of the ionic momenta and positions. Thus, it is valid to use Eq. (22) in liquid metals, and solids at high temperatures.<sup>21</sup>

Intuitively, we feel that Eq. (22) may still be a valid approximation for a solid alloy at low temperatures so long as the collision rate of the electrons is much faster than the Debye frequency  $\omega_D$  of the ionic motion, i. e.,

$$1/\tau \gg \omega_D. \quad (25)$$

This means that the uncertainty in the electron energy is big compared to the maximum phonon energy, so that the conservation of energy in the scattering of one electron by a phonon is of little significance. Under this circumstance we can approximate the phonons as "static scatters" and treat the scattering as elastic as in Eq. (11).

### III. SURVEY

As we have seen in Sec. II, the averaged Green functions  $\langle\langle G \rangle\rangle$  and  $\langle\langle GG \rangle\rangle$  determine the electronic properties of interest in the alloy: the electronic density of states  $\mathfrak{N}(E)$  and the electrical resistivity  $\rho$ . Although there has been some contact between experiment and some aspects of the theory, as reviewed extensively by Mott,<sup>22</sup> plausible approximation schemes for calculations in real disordered materials have not been worked out,<sup>23,24</sup> but are rapidly being developed. In what follows, we shall survey the relevant areas of the field, and state our own problem and methods against this background.

In the averaging process, we must first know the ionic distribution function  $P_c$  in Eq. (14), the quantity that leads to the temperature dependence of the density of states  $\mathfrak{N}(E)$  [Eqs. (16) and (12)], and the conductivity  $\sigma$  [Eq. (21)]. In a completely disordered system with no ionic correlations,  $\langle P_c \rangle_c$  is the trivial uniform distribution

$$\langle P_c \rangle_c = 1/\Omega^N. \quad (26)$$

In this case, there is no temperature variation in  $\mathfrak{N}(E)$ , while the temperature dependence of  $\sigma$  is only characterized by the trivial Fermi distribution factor  $(-df/d\eta)$  in Eq. (21). This uniform distribution is not true even in the most disordered materials like liquid alloys or amorphous material. The determination of the temperature coefficient in  $\mathfrak{N}(E)$  and  $\sigma$  of these materials relies on a genuine understanding of  $P_c$ , which is always complicated. However, when the atomic potential is weak, our

Eqs. (17) or (21) can be reduced<sup>19,25</sup> to the Faber-Ziman-type<sup>26</sup> formula for the resistivity of liquid alloys. What we then need is the structure factor, which can be found from neutron-diffraction experiments or can be calculated as in the work of Bhatia and Thornton.<sup>27</sup> In a crystalline alloy, the ions are restricted to vibrate around their lattice sites. Then the ionic motion can be described in terms of normal modes, or phonons. The average over ionic positions can be replaced by a thermal average over the phonon distribution. In a static-disordered alloy, which is the most popular topic in the literature, the average is simply the configuration average  $\langle \rangle_c$ .

More difficult than the determination of  $P_c$  is the computation of the average in  $\langle\langle G \rangle\rangle$  and  $\langle\langle GG \rangle\rangle$ . The most trivial approximation to  $\langle\langle G \rangle\rangle$  is the one corresponding to  $\langle\langle H \rangle\rangle$ . This sometimes results in a rigid shift of the band, and then is called the "rigid-band" model.<sup>28</sup> In the weak-scattering limit, Edwards,<sup>29</sup> starting from Eq. (17), summed up certain diagrams in both the  $\langle G \rangle_c$  and  $\langle GG \rangle_c$  expansion series and was able to rederive the usual conductivity formula (the one arrived at from the Boltzmann equation). At low concentration, Langer<sup>30</sup> used the many-body thermodynamic Green function<sup>31</sup> and a perturbation expansion to get the conductivity to the first order in concentration. For strong scattering, but localized potentials, Beeby<sup>32</sup> neglected the statistical correlation between the atomic scattering matrices in the multiple scattering expansion of  $\langle G \rangle_c$  and summed up the series to get the so-called "average- $T$ -matrix" approximation. This approximation was somewhat better than earlier ones but still untrustworthy in the concentrated strong-scattering case. Later, Ballentine<sup>33</sup> used a self-consistent method in the calculation of the band structure of liquid Al and Bi. This "self-consistent virtual-crystal" approximation (see Ref. 4) gives no splitting of the alloy band no matter how large the potential strength is. The first good theory to deal with alloys of arbitrary concentrations and scattering strengths is the coherent-potential approximation (CPA). This approach to  $\langle G \rangle_c$  was originated by Soven<sup>8</sup> and was greatly extended by Velický *et al.*<sup>4</sup> Velický<sup>9</sup> further extended CPA to attack the problem of electronic transport in a static alloy, and discussed the numerical results for  $\sigma$  in a model alloy.

So far, the CPA is still the basic working approximation in the electronic theory of concentrated strong-scattering alloys. It is also a powerful tool for other alloy properties. For example, Taylor<sup>34</sup> used the same technique for the lattice vibration problem in alloys, and Onodera and Toyozawa<sup>35</sup> applied the same approximation to Frenkel excitons in mixed ionic crystals. Since we are going to use

CPA in our model calculation of the temperature dependence of  $\Re(E)$  and  $\sigma$  in a crystalline disordered alloy, the CPA formalism will be discussed in detail in the sections that follow.

The more recent developments in the theory of  $\langle\langle G \rangle\rangle$  and  $\langle\langle GG \rangle\rangle$  are either mathematical justifications or generalizations of CPA. First, Yonezawa<sup>36</sup> carefully analyzed and generalized the expansion series in the self-energy of  $\langle G \rangle_c$ . Excluding "multiple occupancy" of a site by more than one atom, she concluded that the approximate self-energy obtainable by summing all terms involving multiple scattering at the same site was identical with the CPA result. Later, Ziman<sup>37</sup> conjectured that for a tight-binding alloy, the "locator" expansion of Matsubara and Toyozawa<sup>38</sup> was superior to the usual band-propagator expansion and used it to arrive at a different conclusion from CPA about the splitting of the band. But in a later paper Leath,<sup>39</sup> using a diagram technique and taking into account the "multiple-occupancy" correction, showed that Ziman's idea was not correct. Furthermore, he also showed that the diagrams of Edwards,<sup>29</sup> Langer,<sup>30</sup> and Verboven,<sup>17</sup> when properly corrected for "multiple occupancy," led to Velický's<sup>9</sup> CPA electrical-conductivity result. In an attempt to improve CPA by including random off-diagonal (hopping) matrix elements, Berk<sup>40</sup> restricted himself to the weak-scattering limit, to avoid the difficulty of the strong-scattering problem. His work is essentially a different version of the "self-consistent virtual-crystal" approximation. An attempt on the same problem was made by Edwards and Loveluck.<sup>41</sup> They used an elaborate diagram method and summed up a large number of diagrams. But their result for the density of states exhibits unphysical band gaps. They also concluded that the self-consistent method was too complicated for their case.

The most substantial generalization of CPA, namely  $CP\vec{n}$ , was recently developed by Freed and Cohen.<sup>42</sup> They generalized the coherent-potential theory from the single-site approximation to  $n$ -atom clusters. The cluster Green function  $G_{\vec{n}}$  (in their notation) is self-consistently determined in a way similar to  $\langle G \rangle_c$  in CPA but more involved. However, they showed that uniformly averaging a finite cluster Green function to get the translationally invariant alloy Green function could not produce a different result from CPA. In order to get nontrivial results, one must go through a subtle averaging process, called  $ECP\vec{n}$  (extended  $CP\vec{n}$  approximation). The simplest version of  $ECP\vec{n}$  is Kohn's notion of periodically compact disordered clusters.<sup>43</sup> The most important results of  $CP\vec{n}$  is the demonstration of the existence of localized states (bound states), outside the CPA band, and in the regions obeying the localization theorem.<sup>44</sup>

Several interesting uses of CPA have appeared in the literature. CPA has not been restricted to the tight-binding approximation. In an early, different version of CPA, Anderson and McMillan<sup>45</sup> used a self-consistent equation for the phase shift to calculate the band structure of liquid iron. Using a similar method, Soven<sup>46</sup> has applied CPA to a muffin-tin potential and has been able to deal with an alloy with constituents of different bandwidths. CPA also serves as an approximate quantitative scheme. It has been used to yield the density of states in Cu-Ni alloys.<sup>5,6</sup> It was also applied to the magnetic properties of Cu-Ni alloys.<sup>47</sup> Velický and Levin<sup>48</sup> have also used CPA to discuss intraband optical constants in a simple tight-binding band. Recently Levin and Ehrenreich<sup>6</sup> applied CPA along with a model Hamiltonian for Ag-Au alloys. By adjusting a concentration-dependent  $d$ -level energy, they could make the concentration dependence of the optical-absorption edge agree with experiment.

From this review, it can be seen that the self-consistent Green function approach to the alloy problem, with CPA as the basic approximation, has been fruitful. Although  $CP\vec{n}$  should give better answers than CPA, at present, when even a model description of  $CP\vec{n}$  has yet to be developed and the  $CP\vec{n}$  two-Green-function average has not even been discussed in the literature, CPA is the only simple and practical method to use in an investigation of the temperature variation trends of  $\Re(E)$  and  $\sigma$  in a concentrated, strong-scattering alloy. It is expected, however, that the method developed below can be generalized to  $CP\vec{n}$ .

#### IV. COHERENT-POTENTIAL APPROXIMATION

Henceforth, we shall consider only crystalline disordered substitutional binary alloys. Let  $x$  and  $y$  be the fractional concentrations of the constituent  $A$  atoms and  $B$  atoms, respectively, so that  $x$  is the probability of an  $A$  atom occupying a given site. The one-electron Hamiltonian  $H$  in Eq. (6) takes the form

$$H = H_0 + U = H_0 + \sum_n U_n, \quad (27)$$

where  $H_0$  is the periodic part of  $H$ , and  $U$  contains the randomness due to both substitutional and thermal disorder.  $U_n$  is the contribution of the  $n$ th site to  $U$ . The decomposition in Eq. (27) is not unique. However, a convenient decomposition can always be chosen for a given system.

Our object is to determine  $\langle\langle G \rangle\rangle$  and  $\langle\langle GG \rangle\rangle$ . Here the double average is a thermal average over the phonon ensemble in a given configuration, followed by an average over all configurations. The coherent-potential approximation (CPA) is a technique for finding a self-consistent solution for the average Green function. The method<sup>49</sup> is outlined below.

The average Green function can be expressed as

$$\langle\langle G(z) \rangle\rangle = \underline{G}(z) = (z - H_0 - \hat{\Sigma})^{-1}. \quad (28)$$

This defines  $\hat{\Sigma}$ , the self-energy operator, which has the full crystal symmetry since  $\underline{G}$  does. Thus  $\hat{\Sigma}$  represents an effective potential for the averaged crystal. Expressing  $G$  from Eq. (18) in terms of  $G$  yields

$$G = \underline{G} + \underline{G}T\underline{G}, \quad (29)$$

where

$$\begin{aligned} T &= (U - \hat{\Sigma})[1 - \underline{G}(U - \hat{\Sigma})]^{-1} = [1 - (U - \hat{\Sigma})\underline{G}]^{-1}(U - \hat{\Sigma}) \\ &= (U - \hat{\Sigma}) + (U - \hat{\Sigma})\underline{G}T. \end{aligned} \quad (30)$$

Now taking the average on both sides of Eq. (29), we get

$$\langle\langle G \rangle\rangle = \underline{G} + \underline{G}\langle\langle T \rangle\rangle \underline{G}, \quad (31)$$

which is solved by

$$\langle\langle T(\hat{\Sigma}) \rangle\rangle = 0. \quad (32)$$

This, as can be seen from Eqs. (28) and (30), is the self-consistent equation which must be solved for  $\hat{\Sigma}$ .  $\hat{\Sigma}$  can be expressed as a sum of self-energy operators  $\hat{\Sigma}_n$ ,

$$\hat{\Sigma} = \sum_n \hat{\Sigma}_n. \quad (33)$$

The choice of the operators  $\hat{\Sigma}_n$  is not unique, the only restriction is that the sum over  $\hat{\Sigma}_n$ 's must add to the operator  $\hat{\Sigma}$  which has the symmetry of the pure crystal. A particular choice will be useful such that each  $\hat{\Sigma}_n$  is localized near its site  $n$  and places an equal contribution on each site.

Since the potential  $U$  is a sum of contributions from each site, i. e.,  $U = \sum_n U_n$ , the scattering operator  $T$  can be expressed as

$$T = \sum_n Q_n = \sum_n \tilde{Q}_n, \quad (34)$$

with

$$\begin{aligned} Q_n &= (U_n - \hat{\Sigma}_n)(1 + \underline{G}T) = T_n \left( 1 + \underline{G} \sum_{m(\neq n)} Q_m \right) \\ &= T_n + \sum_{m(\neq n)} T_n \underline{G} T_m + \sum_{l(\neq m), m(\neq n)} \sum_{m(\neq n)} T_n \underline{G} T_m \underline{G} T_l + \dots, \end{aligned} \quad (35)$$

and

$$\begin{aligned} \tilde{Q}_n &= (1 + T\underline{G})(U_n - \hat{\Sigma}_n) = \left( 1 + \sum_{m(\neq n)} \tilde{Q}_m \underline{G} \right) T_n \\ &= T_n + \sum_{m(\neq n)} T_m \underline{G} T_n + \sum_{l(\neq m), m(\neq n)} \sum_{m(\neq n)} T_l \underline{G} T_m \underline{G} T_n + \dots \end{aligned} \quad (36)$$

The atomic scattering operator  $T_n$  is defined as

$$\begin{aligned} T_n &= (U_n - \hat{\Sigma}_n)[1 - \underline{G}(U_n - \hat{\Sigma}_n)]^{-1} \\ &= (U_n - \hat{\Sigma}_n) + (U_n - \hat{\Sigma}_n)\underline{G}T_n. \end{aligned} \quad (37)$$

In multiple scattering language,  $Q_n$ , as seen from Eqs. (34)–(36), represents the contribution to the

total scattering such that the last scattering happens at site  $n$ ; while  $\tilde{Q}_n$  represents the contribution to the  $T$  such that the first scattering is at site  $n$ . In terms of the  $T_n$ 's, the scattering operator  $T$  has the customary form

$$T = \sum_n T_n + \sum_{\substack{n,m \\ (n \neq m)}} T_n \underline{G} T_m + \sum_{\substack{n,m,l \\ (n \neq m, m \neq l)}} T_n \underline{G} T_m \underline{G} T_l + \dots \quad (38)$$

The ensemble average of Eq. (34) along with Eq. (32) is

$$\langle\langle T \rangle\rangle = \sum_n \langle\langle Q_n \rangle\rangle = \sum_n \langle\langle \tilde{Q}_n \rangle\rangle = 0. \quad (39)$$

But from Eq. (35) we have

$$\langle\langle Q_n \rangle\rangle = \langle\langle T_n (1 + \underline{G} \sum_{m(\neq n)} Q_m) \rangle\rangle. \quad (40)$$

The coherent-potential approximation for  $\hat{\Sigma}$  consists of two ingredients: (i) There exists a decomposition of  $\hat{\Sigma}$  as in Eq. (33) such that we can neglect the statistical correlation between the atomic  $T$  matrix  $T_n$  and the effective waves coming from other sites, i. e.,

$$\begin{aligned} \langle\langle Q_n \rangle\rangle &= \langle\langle T_n (1 + \underline{G} \sum_{m(\neq n)} Q_m) \rangle\rangle \\ &\approx \langle\langle T_n \rangle\rangle (1 + \underline{G} \sum_{m(\neq n)} \langle\langle Q_m \rangle\rangle). \end{aligned} \quad (41)$$

This is a "single-site approximation." (ii)  $\hat{\Sigma}_n$  satisfies

$$\langle\langle T_n(\hat{\Sigma}) \rangle\rangle = 0. \quad (42)$$

Equation (42) is the CPA equation for  $\hat{\Sigma}$ , which entirely determines  $\underline{G}(z)$  and thus the density of states  $\mathcal{N}(E)$ .

For the electrical conductivity, we have to determine the operator  $K$  as defined in Eq. (24). Substituting  $G$  into  $K$  from the Eq. (29), and using the CPA equation, Eq. (32), we can reduce  $K$  to the form

$$K(z_1, p^\alpha, z_2) = \underline{G}(z_1) [p^\alpha + \Gamma(z_1, p^\alpha, z_2)] \underline{G}(z_2), \quad (43)$$

where the vertex operator  $\Gamma$  is given by

$$\Gamma(z_1, p^\alpha, z_2) \equiv \langle\langle T(z_1) \underline{G}(z_1) p^\alpha \underline{G}(z_2) T(z_2) \rangle\rangle. \quad (44)$$

The vertex operator  $\Gamma$  may then be rewritten as the sum of contributions from all sites by using Eq. (34) for  $T$  and Eqs. (35) and (36) for  $Q_n$  and  $\tilde{Q}_n$ , respectively,

$$\begin{aligned} \Gamma &= \sum_n \sum_m \langle\langle Q_n \underline{G} p^\alpha \underline{G} \tilde{Q}_m \rangle\rangle \\ &= \sum_n \sum_m \langle\langle T_n (1 + \underline{G} \sum_{p(\neq n)} Q_p) \underline{G} p^\alpha \underline{G} (1 + \sum_{s(\neq m)} \tilde{Q}_s \underline{G}) T_m \rangle\rangle. \end{aligned} \quad (45)$$

CPA for  $K$  has a further single-site approximation in addition to Eq. (41), i. e.,

$$\langle\langle T_n (1 + \underline{G} \sum_{p(\neq n)} Q_p) \underline{G} p^\alpha \underline{G} (1 + \sum_{s(\neq m)} \tilde{Q}_s \underline{G}) T_m \rangle\rangle$$

$$\simeq \langle \langle T_n \langle \langle (1 + \underline{G} \sum_{p(\neq n)} Q_p) \underline{G} p^\alpha \underline{G} (1 + \sum_{s(\neq m)} \tilde{Q}_s \underline{G}) \rangle \rangle T_m \rangle \rangle, \quad (46)$$

which is zero for  $n \neq m$ , since  $T_n$  and  $T_m$  are then independent, and each averages to zero, by Eq. (42). Thus we arrive at the following result:

$$\begin{aligned} \langle \langle Q_n \underline{G} p^\alpha \underline{G} \tilde{Q}_m \rangle \rangle &\simeq \langle \langle Q_n \underline{G} p^\alpha \underline{G} \tilde{Q}_n \rangle \rangle \delta_{nm} \\ &\equiv \Gamma_n \delta_{nm}. \end{aligned} \quad (47)$$

This, in two-resolvent language, means that we have neglected all the statistical correlations between two particles unless they are scattered at the same site. In other words, we have neglected the statistical correlation between the scattered waves from two different sites.

Using Eqs. (35), (36), and (46) we find

$$\begin{aligned} \Gamma_n &= \langle \langle Q_n \underline{G} p^\alpha \underline{G} \tilde{Q}_n \rangle \rangle \\ &\simeq \langle \langle T_n \langle \langle (1 + \underline{G} \sum_{p(\neq n)} Q_p) \underline{G} p^\alpha \underline{G} (1 + \sum_{s(\neq n)} \tilde{Q}_s \underline{G}) \rangle \rangle T_n \rangle \rangle \\ &= \langle \langle T_n \langle \langle \underline{G} p^\alpha \underline{G} + \underline{G} (\sum_{p(\neq n)} \langle \langle Q_p \underline{G} p^\alpha \underline{G} \tilde{Q}_p \rangle \rangle) \underline{G} \rangle \rangle T_n \rangle \rangle \\ &= \langle \langle T_n \underline{G} (p^\alpha + \sum_{p(\neq n)} \Gamma_p) \underline{G} T_n \rangle \rangle. \end{aligned} \quad (48)$$

In Eq. (48) we have used the CPA results  $\langle \langle Q_n \rangle \rangle = \langle \langle \tilde{Q}_n \rangle \rangle = 0$ .

Combine Eqs. (43), (45), (47), and (48) to obtain the closed equations for  $K$ ,

$$K = \underline{G} (p^\alpha + \sum_n \Gamma_n) \underline{G}, \quad (49)$$

and

$$\Gamma_n = \langle \langle T_n K T_n \rangle \rangle - \langle \langle T_n \underline{G} \Gamma_n \underline{G} T_n \rangle \rangle, \quad (50)$$

which yield the formal solution for  $\Gamma$ :

$$\begin{aligned} \Gamma &= \sum_n \langle \langle T_n \underline{G} p^\alpha \underline{G} T_n \rangle \rangle \\ &+ \sum_{\substack{n, m \\ (n \neq m)}} \langle \langle T_n \underline{G} \langle \langle T_m \underline{G} p^\alpha \underline{G} T_m \rangle \rangle \underline{G} T_n \rangle \rangle + \dots \end{aligned} \quad (51)$$

Equations (49) and (50) complete the CPA formalism. They are still formidable. We have to obtain the self-energy from Eq. (42) in order to get  $\underline{G}$ , then try to sum the series in Eq. (51) to get  $\Gamma$ , and finally insert  $\Gamma$  into Eq. (43) to find  $K$ . In Sec. V A a simple band model Hamiltonian will be used to reduce the operator equations to simple scalar equations.

## V. MODEL CALCULATION

### A. Simple Band Model

We shall use the simplest possible model electron Hamiltonian that includes both substitutional impurities and thermal disorder,

$$H = H_0 + D + \Theta, \quad (52)$$

where

$$H_0 = \sum'_{n, m} |n\rangle t_{nm} \langle m| \quad (53)$$

represents the part of the Hamiltonian off-diagonal in site indices, and the  $t_{nm}$  are assumed to be periodic, and independent of alloying and lattice distortion,

$$D = \sum_n |n\rangle \mathcal{E}_n \langle n| \quad (54)$$

represents the "impurity" Hamiltonian with  $\mathcal{E}_n$  either  $\mathcal{E}_A$  or  $\mathcal{E}_B$ , according to whether an  $A$  or  $B$  atom is on site  $n$ , and

$$\Theta = \sum_n |n\rangle \theta_n \langle n| \quad (55)$$

is the electron-phonon interaction. The phonon operator  $\theta_n$  depends on which ion occupies site  $n$  and on the phonon coordinates. This model is a generalization of the Koster-Slater one-impurity case, and is identical with the model exploited by Velický *et al.*,<sup>4</sup> with the addition of the phonon contribution.

A few words are appropriate here about some assumptions, definitions, and redefinitions that we are making. Some of the problems about which we shall be speaking are already present in the Koster-Slater case, although they are customarily (and unnecessarily) ignored. The heart of the problem is the definition of the site basis and implications of the choice. Let us take  $|n\rangle$  to be an atomic or Wannier function centered at  $\vec{R}_n^0$ . Following the convenient custom, we pretend that the  $\{|n\rangle\}$  are not only very localized, as are atomic wave functions, but also orthogonal, as are Wannier functions. In other words, we assume that the difference between Wannier and atomic wave functions can be neglected, as is true in a good tight-binding case. Now usually, in an exposition of the Koster-Slater model, the  $\{|n\rangle\}$  are all taken to be one type of wave functions, e.g., pure  $A$ -crystal Wannier functions associated with a single atomic orbital, but this is highly unphysical—the true wave function cannot generally be approximated well on such a basis without multiplying the number of bands taken into account. Therefore, let us initially take  $|n\rangle$  to be  $|n_A\rangle$  or  $|n_B\rangle$ , the state appropriate to the type of atom at the site  $n$ ,  $|n\rangle$  being centered on the actual position  $\vec{R}_n$ , rather than the official lattice position  $\vec{R}_n^0$ . We assume that the tails of the atomic basis are almost the same, so that we can neglect differences in the off-diagonal matrix elements of energy and momentum  $t_{nm}$  and  $\vec{p}_{nm}$  and assume them to be independent of alloying. The phonon contribution is restricted to be diagonal only for the resulting mathematical convenience in the CPA formalism.

Now let us redefine our point of view or notation. Using the basis described above, for a particular configuration, let us convert all operators, such as  $G$ ,  $K$ , etc., into matrices, and regard all the CPA equations as matrix equations. Equivalently, we could turn these matrices into operators by using

an abstract periodic basis. The final results will not be affected, of course, but some very clumsy notation and language is being avoided, without pretending that Schrödinger's equation is insensitive to the potential (the literal use of one type of  $|n\rangle$ ).

Let us apply the CPA formulation of Sec. IV to the simple band model. In the "mock-periodic" crystal described by  $H_0$ , the Green function is

$$G_0(z) = (z - H_0)^{-1} = \sum_{\vec{k}} \frac{|\vec{k}\rangle\langle\vec{k}|}{z - \epsilon(\vec{k})}, \quad (56)$$

where the  $|\vec{k}\rangle$  are the "mock Bloch states" of  $H_0$  defined by

$$|\vec{k}\rangle \equiv (1/N^{1/2}) \sum_n e^{i\vec{k}\cdot\vec{R}_n^0} |n\rangle, \quad (57)$$

with energy  $\epsilon(\vec{k})$  given by the usual expression

$$\epsilon(\vec{k}) = \sum_n e^{i\vec{k}\cdot\vec{R}_n^0} t_{n0}, \quad (58)$$

and  $\vec{k}$  is the usual wave vector in the Brillouin zone associated with the static crystal lattice. The Wannier or atomic states  $|n\rangle$  of the site basis are then related to the "mock Bloch states" by

$$|n\rangle = (1/N^{1/2}) \sum_{\vec{k}} e^{-i\vec{k}\cdot\vec{R}_n^0} |\vec{k}\rangle. \quad (59)$$

Since the site-diagonal matrix elements of  $G_0$  are site independent, i. e.,

$$\begin{aligned} F_0(z) &\equiv \langle n | G_0(z) | n \rangle = \langle 0 | G_0(z) | 0 \rangle \\ &= \frac{1}{N} \sum_{\vec{k}} \frac{1}{z - \epsilon(\vec{k})}, \end{aligned} \quad (60)$$

the pure crystal density of states per atom,  $\mathfrak{A}_0$ , according to Eq. (20), is

$$\mathfrak{A}_0(E) = \pm (1/\pi) \text{Im} F_0(E \mp i0). \quad (61)$$

Another useful relation between  $F_0$  and  $\mathfrak{A}_0$ , obtainable from Eq. (60), is

$$F_0(z) = \int dE \mathfrak{A}_0(E) / (z - E). \quad (62)$$

The averaged finite-temperature alloy described by  $\underline{G}(z)$  has the full crystal symmetry. Thus, corresponding to Eq. (60), we can define

$$F(z) \equiv \langle 0 | \underline{G}(z) | 0 \rangle = \frac{1}{N} \sum_{\vec{k}} \frac{1}{z - \epsilon(\vec{k}) - \Sigma(z, \vec{k})}. \quad (63)$$

Here we have used Eq. (28) and the general periodic property of the self-energy,

$$\hat{\Sigma}(z) = \sum_{\vec{k}} |\vec{k}\rangle \Sigma(z, \vec{k}) \langle \vec{k}|. \quad (64)$$

In the coherent-potential approximation we obtain the self-energy from the solution of Eq. (42). A scalar solution for  $\hat{\Sigma}$  can be found, so that the self-energy is a sum of site contributions, i. e.,

$$\hat{\Sigma}_n = |n\rangle \Sigma \langle n|. \quad (65)$$

Thus,  $T_n$  [Eq. (37)] is site diagonal, and the op-

erator equation, Eq. (42), becomes the scalar equation

$$\left\langle \left\langle \frac{\mathcal{G}_n + \theta_n - \Sigma}{1 - (\mathcal{G}_n + \theta_n - \Sigma)F} \right\rangle \right\rangle = 0. \quad (66)$$

This equation for  $\Sigma$  reduces to Eq. (22) of Ref. 4, if  $\theta_n \rightarrow 0$ , i. e., in the static alloy. However, in the static alloy the equation for  $\Sigma$  is merely algebraic, whereas here, with phonons included, it is an integral equation.

Once we obtain  $\Sigma$  from Eq. (66), we can obtain  $F$  from Eq. (63) in terms of  $F_0$  [see Eq. (60)],

$$F(z) = F_0(z - \Sigma), \quad (67)$$

since  $\Sigma$  is independent of  $\vec{k}$ . The density of states per atom  $\mathfrak{A}(E)$  is then, from Eqs. (20) and (63),

$$\mathfrak{A}(E) = \pm (1/\pi) \text{Im} F(E \mp i0). \quad (68)$$

To obtain an expression for the conductivity, we first prove that the vertex correction  $\Gamma$  in Eq. (51) vanishes. Each term in the series expansion, Eq. (51), contains a factor  $T_n \underline{G} p^\alpha \underline{G} T_n$ . Since  $T_n$  is site diagonal,  $\Gamma = 0$ , if  $\langle n | \underline{G} p^\alpha \underline{G} | n \rangle = 0$ . But we have

$$\begin{aligned} \langle n | \underline{G} p^\alpha \underline{G} | n \rangle &= \frac{1}{N} \sum_{\vec{k}} \frac{m v^\alpha(\vec{k})}{[z_1 - \epsilon(\vec{k}) - \Sigma(z_1)][z_2 - \epsilon(\vec{k}) - \Sigma(z_2)]}, \end{aligned} \quad (69)$$

where  $v^\alpha(\vec{k})$  is the  $\alpha$  component of the velocity, defined by

$$v^\alpha(\vec{k}) \equiv (1/m) \langle \vec{k} | p^\alpha | \vec{k} \rangle. \quad (70)$$

Time-reversal symmetry gives the relations

$$v^\alpha(-\vec{k}) = -v^\alpha(\vec{k}), \quad (71)$$

and

$$\epsilon(-\vec{k}) = \epsilon(\vec{k}). \quad (72)$$

Therefore, the summation in Eq. (69) vanishes identically. Thus, from Eq. (49),

$$K = \underline{G} p^\alpha \underline{G}. \quad (73)$$

Combining Eqs. (22), (23), (70), and (73), and defining  $g(\vec{k}, z)$  as

$$g(\vec{k}, z) \equiv \langle \vec{k} | \underline{G}(z) | \vec{k} \rangle = [z - \epsilon(\vec{k}) - \Sigma(z)]^{-1}, \quad (74)$$

the conductivity becomes

$$\sigma^{\alpha\beta} = \frac{2e^2\hbar}{\pi\Omega} \int d\eta \left( -\frac{d\eta}{d\eta} \right) \sum_{\vec{k}} v^\alpha(\vec{k}) v^\beta(\vec{k}) [\text{Im} g(\vec{k}, \eta^*)]^2. \quad (75)$$

Or, following Velický,<sup>50</sup> we have the alternate form

$$\sigma^{\alpha\beta} = \frac{2e^2\hbar}{\pi\Omega_c} \int d\eta \left( -\frac{d\eta}{d\eta} \right) \int d\xi \left( \frac{\Delta(\eta)}{[\eta - \xi - \Lambda(\eta)]^2 + \Delta^2(\eta)} \right)^2$$



$$\times \frac{1}{N} \sum_{\mathbf{k}} v^{\alpha}(\mathbf{k}) v^{\beta}(\mathbf{k}) \delta(\xi - \epsilon(\mathbf{k})) , \quad (76)$$

where  $\Omega_c$  is the volume per atom and  $\Lambda$  and  $\Delta$  are defined from the self-energy  $\Sigma$ ,

$$\Lambda(\eta) \equiv \text{Re}\Sigma(\eta \pm i0) , \quad (77)$$

and

$$\Delta(\eta) \equiv |\text{Im}\Sigma(\eta \pm i0)| . \quad (78)$$

We have now set down the expressions for the model Hamiltonian conductivity and density of states. In Sec. VB, we shall discuss the phonon system and the phonon averaging process in the self-energy equation, (66).

#### B. Electron-Phonon Interaction and Distribution Function for $\theta_n$

In the harmonic approximation, the atomic motion of the alloy in a given configuration can be described by the Hamiltonian

$$H_{\text{ph}} = \sum_{s=1}^{3N} \hbar \omega_s \left( \frac{1}{2} + b_s^{\dagger} b_s \right) , \quad (79)$$

where  $b_s^{\dagger}$  and  $b_s$  are the creation and destruction operators for a phonon in states, with frequency  $\omega_s$ . However, in a concentrated alloy the phonon quantum number  $s$  can no longer be identified with the crystal momentum. The electron-phonon interaction, which does not conserve crystal momentum, is represented in our model [Eq. (55)] by the local Hamiltonian

$$H_{\text{ep}} = \Theta = \sum_n |n\rangle \theta_n \langle n| . \quad (80)$$

We make the standard, excellent approximation<sup>51</sup>

$$\theta_n = \sum_s [\gamma_s(n) b_s + \gamma_s^*(n) b_s^{\dagger}] , \quad (81)$$

where  $\gamma_s(n)$  is the coupling constant for an electron at the  $n$ th site to absorb a phonon with quantum number  $s$ . Notice that  $\gamma_s(n)$ ,  $b_s$ , and  $\theta_n$  are configuration dependent. Notice also that since  $\theta_n$  is an operator, the self-consistent equation, Eq. (66), is a phonon-operator equation. However we can reduce it to a scalar form as follows.

The phonon average of any function  $f(\theta_n)$  of the operator  $\theta_n$  is

$$\langle f(\theta_n) \rangle_{\text{p}} = \text{Tr}_{\text{ph}} [\rho_{\text{ph}} f(\theta_n)] , \quad (82)$$

where

$$\rho_{\text{ph}} = e^{-\beta H_{\text{ph}}} \{ \text{Tr}_{\text{ph}} [e^{-\beta H_{\text{ph}}}] \}^{-1} , \quad (83)$$

and the trace is over all states of the lattice motion. The average  $\langle f(\theta_n) \rangle_{\text{p}}$  can also be written in terms of the probability distribution  $P_n(\eta)$  as

$$\langle f(\theta_n) \rangle_{\text{p}} = \int d\eta f(\eta) P_n(\eta) , \quad (84)$$

where  $P_n(\eta)$  is defined in terms of its characteristic function  $\varphi_n(\lambda)$ ,

$$P_n(\eta) = (1/2\pi) \int d\lambda e^{-i\lambda\eta} \varphi_n(\lambda) , \quad (85)$$

which in turn is defined as

$$\varphi_n(\lambda) = \text{Tr}_{\text{ph}} [\rho_{\text{ph}} e^{i\lambda\theta_n}] . \quad (86)$$

Explicitly, the characteristic function is

$$\varphi(\lambda) = \text{Tr}_{\text{ph}} \{ \exp[-\beta \sum_s \hbar \omega_s (\frac{1}{2} + b_s^{\dagger} b_s)] \exp[i\lambda \sum_s (\gamma_s(n) b_s + \gamma_s^*(n) b_s^{\dagger})] \} \{ \text{Tr}_{\text{ph}} [\exp(-\beta \sum_s \hbar \omega_s (\frac{1}{2} + b_s^{\dagger} b_s)) ] \}^{-1} \quad (87)$$

$$= \text{Tr}_{\text{ph}} \{ (\prod_s \rho_s) \prod_s \exp[i\lambda (\gamma_s(n) b_s + \gamma_s^*(n) b_s^{\dagger})] \} \quad (88)$$

$$= \prod_s \{ \text{Tr}_{\text{ph}} [\rho_s e^{i\lambda \hat{q}_s^{(n)}}] \} \equiv \prod_s \varphi_n^{(s)}(\lambda) . \quad (89)$$

In the above expression, we have defined

$$\rho_s \equiv \exp[-\beta \hbar \omega_s (\frac{1}{2} + b_s^{\dagger} b_s)] \left( \sum_{n=1}^{\infty} \exp[-\beta \hbar \omega_s (\frac{1}{2} + n)] \right)^{-1} , \quad (90)$$

and

$$\hat{q}_s(n) \equiv \gamma_s(n) b_s + \gamma_s^*(n) b_s^{\dagger} , \quad (91)$$

and have used the commutation relation

$$[\rho_s, \hat{q}_{s'}(n)] = 0 , \quad s \neq s' . \quad (92)$$

Note  $\varphi_n^{(s)}(\lambda)$  is the characteristic function of  $\hat{q}_s(n)$ , which is essentially the displacement of a one-dimensional quantum oscillator, so that we use the standard result<sup>52</sup>

$$\varphi_n^{(s)}(\lambda) = e^{-\alpha_n^{(s)} \lambda^2 / 2} , \quad (93)$$

where

$$\alpha_n^{(s)} = |\gamma_s(n)|^2 \coth(\frac{1}{2} \beta \hbar \omega_s) . \quad (94)$$

Note that  $\alpha_n^{(s)}$  is proportional to the Debye-Waller factor times the square of the electron-phonon coupling constant. Since the characteristic function  $\varphi_n(\lambda)$  is a Gaussian, its Fourier transform, the distribution function, is a Gaussian too. Thus the distribution function is

$$P_n(\eta) = (2\pi\alpha_n)^{-1/2} e^{-\eta^2/2\alpha_n} . \quad (95)$$

Applying Eqs. (84) and (95) to the self-consistent equation (66), we have a scalar integral equation for  $\Sigma$ ,

$$\int d\eta \left\langle (2\pi\alpha_n)^{-1/2} e^{-\eta^2/2\alpha_n} \left( \frac{\mathcal{E}_n + \eta - \Sigma}{1 - (\mathcal{E}_n + \eta - \Sigma)F} \right) \right\rangle_c = 0 . \quad (96)$$

Let us define a local distribution  $P_A(\eta)$ , which is the average of  $P_n(\eta)$  over all configurations with an  $A$  atom at the  $n$ th site, and define  $P_B(\eta)$  similarly. Then Eq. (96) becomes more explicit,

$$\int d\eta \left( x P_A(\eta) \frac{\mathcal{E}_A + \eta - \Sigma}{1 - (\mathcal{E}_A + \eta - \Sigma)F} + y P_B(\eta) \frac{\mathcal{E}_B + \eta - \Sigma}{1 - (\mathcal{E}_B + \eta - \Sigma)F} \right) = 0. \quad (97)$$

The equation for  $\Sigma$  thus depends on the pure crystal density of states and the distribution function. In Sec. V C we shall further simplify the model in order to get a qualitative idea of the temperature dependence of quantity of states and the conductivity.

### C. Model Density of States, Velocity-Dispersion, and Local-Distribution Functions

Let us first review the procedure for calculating the self-energy  $\Sigma$ , the density of states  $\mathfrak{N}$ , and the conductivity  $\sigma$ , and then describe some model functions that we have actually used in our computations.

To calculate the self-energy  $\Sigma$ , we need to (i) obtain  $F_0(z)$  from the dispersion relation  $\epsilon(\vec{k})$ , using Eq. (60), or from the pure crystal density of states  $\mathfrak{N}_0(E)$ , using Eq. (62); (ii) express  $F$  as a function of  $\Sigma$  by Eq. (67); (iii) specify the electron-phonon parameter  $\gamma_s(n)$ , then get  $\alpha_n$  from Eq. (94), and perform the configuration average on  $P_n(\eta)$  to get  $P_A(\eta)$  and  $P_B(\eta)$ ; (iv) solve the integral equation (97) for  $\Sigma$ .

Once the self-energy is obtained, we compute the density of states  $\mathfrak{N}(E)$  from Eq. (68).

To compute the conductivity, we assume a cubic lattice, so that the averaged conductivity is isotropic,

$$\sigma^{\alpha\beta} = \sigma \delta_{\alpha\beta}, \quad (98)$$

where, according to Eq. (76),

$$\sigma = \frac{2e^2\hbar}{\pi\Omega_c} \int d\eta \left( -\frac{df}{d\eta} \right) \int d\xi \left[ \left( \frac{\Delta(\eta)}{(\eta - \Lambda(\eta) - \xi)^2 + \Delta^2(\eta)} \right)^2 \times \frac{1}{3N} \sum_{\vec{k}} v^2(\vec{k}) \delta(\xi - \epsilon(\vec{k})) \right]. \quad (99)$$

If we define the velocity dispersion  $v(\epsilon)$  by

$$v^2(\epsilon) \equiv [1/N \mathfrak{N}_0(E)] \sum_{\vec{k}} v^2(\vec{k}) \delta(\epsilon - \epsilon(\vec{k})), \quad (100)$$

then

$$\sigma = \frac{2e^2\hbar}{3\pi\Omega_c} \int d\eta \left( -\frac{df}{d\eta} \right) \int d\xi \frac{v^2(\xi) \mathfrak{N}_0(\xi) \Delta^2(\eta)}{[(\eta - \Lambda(\eta) - \xi)^2 + \Delta^2(\eta)]^2}. \quad (101)$$

Since we are investigating the general trends, it is neither convenient nor profitable to start our calculation from a detailed  $\epsilon(\vec{k})$  and  $\gamma_s(n)$ . Instead, we shall use simple model forms for  $\mathfrak{N}_0(E)$ ,  $v^2(E)$ , and local distributions  $P_A$  and  $P_B$  as follows.

For pure crystal density of states, we have adopted the Hubbard<sup>53</sup> ellipse model,

$$\mathfrak{N}(E) = \begin{cases} (2/\pi)(1 - E^2)^{1/2}, & |E| \leq 1 \\ 0, & |E| > 1 \end{cases} \quad (102)$$

where the energy unit is a half-bandwidth  $w$ . This model is essentially an approximation to a simple cubic tight-binding  $s$ -band density of states. It also behaves like a free-electron density of states around the bottom of the band. This is a model that has been used extensively in calculations of electronic properties in alloys.<sup>4</sup>

Corresponding to Eq. (102), we have

$$F_0(z) = 2z - 2(z^2 - 1)^{1/2}, \quad (103)$$

so that

$$F(z) = F_0(z - \Sigma) = 2(z - \Sigma) - 2[(z - \Sigma)^2 - 1]^{1/2}. \quad (104)$$

The simplest form for the local distribution functions  $P_A$  and  $P_B$  can be obtained by assuming that the electron-phonon interaction is independent of configurations,

$$P_A(\eta) = P_B(\eta) = (2\pi\alpha)^{-1/2} e^{-\eta^2/2\alpha}. \quad (105)$$

Instead, and intuitively more attractive, we take

$$P_{A,B}(\eta) = (2\pi\alpha_{A,B})^{1/2} e^{-\eta^2/2\alpha_{A,B}}, \quad (106)$$

which could, for example, be obtained by taking a typical term in the configuration average leading to  $P_A$  and  $P_B$ . The input parameters  $\alpha_A$  and  $\alpha_B$  are linear in temperature at high temperatures [see Eq. (94)]. Rough estimates of  $\alpha$  values can be found in Appendix A.

The spectrum  $\epsilon(\vec{k})$ , and therefore  $v^2(E)$ , cannot be uniquely derived from  $\mathfrak{N}_0(E)$ . Following Velický,<sup>9</sup> we chose the form

$$v^2(E) = v_m^2(1 - E^2), \quad (107)$$

which corresponds well with our model  $\mathfrak{N}_0(E)$ , and with the simple band structure we just mentioned.

Here  $v_m$  is the maximum velocity in the band.

Combining Eqs. (101), (102), and (107), we obtain

$$\sigma = \frac{4e^2\hbar v_m^2}{3\pi^2\Omega_c} \int d\eta \left( -\frac{df}{d\eta} \right) \int_{-1}^1 d\xi \times \frac{\Delta^2(\eta)(1 - \xi^2)^{3/2}}{\{[\eta - \xi - \Lambda(\eta)]^2 + \Delta^2(\eta)\}^2}. \quad (108)$$

For later convenience, let us define a function  $\mathcal{L}(\eta)$  by

$$\mathcal{L}(\eta) \equiv \int_{-1}^1 d\xi (1 - \xi^2) \frac{\Delta^2(\eta)}{\{[\eta - \xi - \Lambda(\eta)]^2 + \Delta^2(\eta)\}^2}, \quad (109)$$

or, after integration (see Appendix B),

$$\mathcal{L}(\eta) = \frac{\pi^4 \mathfrak{N}^3(\eta)}{16\Delta(\eta)} \left( 1 + \frac{6\Delta(\eta)}{\pi \mathfrak{N}(\eta)} \right). \quad (110)$$

For a metal alloy,  $(-df/d\eta)$  is a sharply peaked function of  $\eta$  at the Fermi energy  $\eta = \epsilon_F$ , and we can then express  $\sigma$  in the usual approximation

$$\sigma = \frac{4e^2\hbar v_m^2}{3\pi^2\Omega_c} [\mathcal{L}(\epsilon_F) + \frac{1}{3}\pi^2\mathcal{L}''(\epsilon_F)(\kappa T)^2 + \dots] \quad (111)$$

Since  $\mathcal{L}(\eta)$  is a smooth function of  $\eta$  except at the singular points of the density of states, terms involving  $\mathcal{L}''(\epsilon_F)$  and higher derivatives are small compared to  $\mathcal{L}(\epsilon_F)$  and may be neglected. Thus, if  $\epsilon_F$  is not too close to a band edge, or other singularity, it is sufficient to keep only the first term in the expansion of Eq. (111), so the conductivity becomes

$$\sigma = \frac{\pi^2 e^2 \hbar v_m^2}{12\Omega_c} \frac{\mathcal{N}^3(\epsilon_F)}{\Delta(\epsilon_F)} \left( 1 + \frac{6\Delta(\epsilon_F)}{\pi\mathcal{N}(\epsilon_F)} \right) \quad (112)$$

The temperature dependence of the density of states and the conductivity can now be investigated. The details and results of numerical calculation will be presented in Sec. VD. However, a quicker understanding of some features of this theory can be obtained by investigating the weak-scattering limit. This topic is treated in Appendix C.

#### D. Computational Procedures

Let us review the input parameters needed for the computation. For a binary alloy  $A_x B_y$  at finite temperature  $T$ ,  $x$  and  $y$  are the concentrations of  $A$  and  $B$  atoms,  $\mathcal{E}_A$  and  $\mathcal{E}_B$  are the strengths of static random potentials around  $A$  and  $B$  atoms, respectively, and,  $\alpha_A$  and  $\alpha_B$  are the electron-phonon interaction parameters which are linear in temperature at high temperatures. Indeed,  $\alpha_A$  and  $\alpha_B$  can be thought of as the mean square of the thermal fluctuation in the atomic-potential strengths  $\mathcal{E}_A$  and  $\mathcal{E}_B$ , respectively. It is convenient to define the origin of energy and a scattering strength  $\delta$  by

$$\mathcal{E}_A = \frac{1}{2}\delta, \quad \mathcal{E}_B = -\frac{1}{2}\delta \quad (113)$$

Here all the energies are in units of the half-bandwidth.

To solve for  $\Sigma$  from the integral equation (97), it is convenient to express it in a different form which is useful for iteration,

$$\Sigma = \left\langle \left\langle \frac{\mathcal{E}_n + \theta_n}{1 - (\mathcal{E}_n + \theta_n - \Sigma)F} \right\rangle \right\rangle \left\langle \left\langle \frac{1}{1 - (\mathcal{E}_n + \theta_n - \Sigma)F} \right\rangle \right\rangle^{-1}, \quad (114)$$

which can be simplified further to

$$\Sigma = z - \frac{1}{4}F - \left\langle \left\langle \frac{1}{z - (\mathcal{E}_n + \theta_n) - \frac{1}{4}F} \right\rangle \right\rangle^{-1} \quad (115)$$

In deriving Eq. (115), we have used Eq. (104), which can be rewritten as

$$\Sigma = z - 1/F(z) - \frac{1}{4}F(z) \quad (116)$$

The iteration procedure is as follows. Start with some appropriate  $F$ , compute  $\Sigma$  from Eq. (115), which provides a new  $F$  from Eq. (104), and so on.

The convergence of  $\Sigma$  depends on a good choice for the initial  $F$ . Notice that  $F$  is the site-diagonal matrix element of a translationally invariant Green function. In iterating, good convergence tends to depend on starting out close to the final answer. Since the phonons usually have a small effect compared with the alloying, the best initial trial value to use for  $F$  is generally the static alloy  $F^{(0)}$ . The speed of convergence also depends on the energy. There is always better convergence at the band center than at the band edges. So, in the actual computation, we solve for the static alloy  $F^{(0)}$  (to be discussed shortly), then we start iterating at an energy corresponding to the peak of the static density of states, iterating Eq. (115) to get the temperature-dependent self-energy  $\Sigma$  at that energy. Then we use this  $\Sigma$  or the corresponding  $F$  as the initial value for a neighboring energy, and continue this procedure to the tails of the band. In the case of split bands, we carry out the procedure for each subband separately. The self-energy  $\Sigma^{(0)}$  and the corresponding  $F^{(0)}$  of the static alloy have been discussed in detail in Ref. 4. Here we only quote the results of Ref. 4 whenever they are needed for our computation. It is convenient to solve for  $F^{(0)}$ , which satisfies a cubic equation,

$$\frac{1}{16}(F^{(0)})^3 - \frac{1}{2}z(F^{(0)})^2 + [z^2 - \frac{1}{4}(\delta^2 - 1)](F^{(0)}) - (z + \bar{\epsilon}) = 0, \quad (117)$$

where  $\bar{\epsilon}$  is the averaged energy  $x\mathcal{E}_A + y\mathcal{E}_B$ . When Eq. (117) is solved for a real energy  $z = E$  in the band, there are three roots. We only choose the correct root corresponding to  $z = E + i0$ , i. e., the imaginary part of  $F^{(0)}$  must be negative in order to give a positive density of states [see Eq. (68)].

In the process of iteration in Eq. (115), we always encounter the following average:

$$\begin{aligned} & \langle \langle [z - (\mathcal{E}_n + \theta_n) - \frac{1}{4}F]^{-1} \rangle \rangle \\ &= \int d\eta \left( \frac{x}{(2\pi\alpha_A)^{1/2}} e^{-\eta^2/2\alpha_A} (z - \mathcal{E}_A - \eta - \frac{1}{4}F)^{-1} \right. \\ & \quad \left. + \frac{y}{(2\pi\alpha_B)^{1/2}} e^{-\eta^2/2\alpha_B} (z - \mathcal{E}_B - \eta - \frac{1}{4}F)^{-1} \right) \\ &= (1/\pi^{1/2}) \int dt e^{-t^2} \{ x [z - \mathcal{E}_A - (2\alpha_A)^{1/2}t]^{-1} \} \end{aligned}$$

$$+y[z - \mathcal{E}_B - (2\alpha_B)^{1/2}t]^{-1} \}. \quad (118)$$

In other words, we have to carry out the integration

$$W(z_{A,B}) \equiv \int dt \frac{e^{-t^2}}{z_{A,B} - t}, \quad (119)$$

where

$$z_{A,B} = \frac{1}{(2\alpha_{A,B})^{1/2}} (z - \mathcal{E}_{A,B} - \frac{1}{4}F). \quad (120)$$

Since, for a real energy  $z = E$  in the band,  $F$  will have a negative imaginary part, we have

$$\text{Im } z_{A,B} > 0. \quad (121)$$

Except for a constant, the integral in Eq. (119), is a complex error function. A discussion of this function and the tabulated values for certain ranges of the argument are given in Ref. 54. In the actual calculation, we used the series expansion<sup>55</sup> for  $|\text{Re } z_{A,B}| \leq 2.8$  and  $|\text{Im } z_{A,B}| \leq 1.4$ , while outside this range we used the ten-point Gaussian-Hermite quadrature formula.<sup>56</sup> The convergence for most cases is very fast.

Once the self-energies inside the bands are obtained,  $F$  follows immediately, yielding in its turn the density of states from Eq. (68). It is then easy to obtain the conductivity as a function of the Fermi energy, since we have expressed the conductivity in terms of the density of states and self-energy [see Eq. (112)]. But if we want the conductivity as a function of temperature, we have to calculate the Fermi level at each temperature. This can be done by solving for  $\epsilon_F$  in

$$c = 2 \int_{-\infty}^{\infty} d\epsilon f(\epsilon) \mathfrak{N}(\epsilon) \approx 2 \int_{-\infty}^{\epsilon_F} d\epsilon \mathfrak{N}(\epsilon), \quad (122)$$

where  $c$  is the average number of electrons per alloy atom and is given by

$$c = xC_A + yC_B. \quad (123)$$

Here  $C_A$  and  $C_B$  are numbers of electrons per atom for pure  $A$  and  $B$  crystals.

#### E. Results of Numerical Calculations and Discussion

Because we do not have a definite alloy in mind, all the parameters are free to vary for different alloys. We shall only pick some representative values for each parameter for numerical illustrations. However, an understanding of salient features of these examples should give some insight into the nature of the model.

In Fig. 1(a)–(c), the self-energy is plotted as a function of energy. Each figure represents an alloy with a definite concentration  $x$  and scattering strength  $\delta$  but at two different temperatures. The solid line represents the static alloy while the dashed line stands for the alloy at  $T \neq 0$ . Figure

1(a) represents an alloy in the virtual-crystal limit, in which  $x = 0.1$ ,  $\delta = 0.5$ . We shall refer to a situation as having “virtual-crystal” character when  $\delta$  is small, and  $\Sigma$  relatively slowly varying (so that perturbation theory is reasonable). The scattering nature of the static alloy is characterized by a hump of  $\Delta$  at the top of the band. When thermal disorder is introduced,  $\Delta$  increases in the whole range of energy inside the band. But the increase of  $\Delta$  in the lower-energy part of the band is greater than that around the hump of the static  $\Delta$ , in contrast with the usual proportionality to the density of states [see Fig. 2(a)]. The real part of the self-energy  $\Lambda$  of the static alloy is almost a constant in the lower part of the band, but has interesting structure in the “impurity” part of the band. The thermal disorder affects the “host” part and “impurity” part equally, so that we have a shift of the spectrum from the center of each component band to both wings. This is reflected in the change of  $\Lambda$ . As we go from the lower-energy region up to higher-energy, we have a negative change in  $\Lambda$ , then a positive change, then the change in  $\Lambda$  tends to become negative when we enter the impurity part, and finally positive at the very top of the band. In Fig. 1(b), where  $x = 0.5$ ,  $\delta = 0.8$ , the alloy is concentrated, and the scattering strength is moderately large. The static-alloy  $\Delta$  has a very sharp peak at the center of the band where the impurity scattering is most effective. The thermal disorder causes a positive change in both wings of the band but a negative change at the center. The decreases in  $\Delta$  happen at the energies corresponding to the strongest damping in the static alloy. As will be clear from our later discussion of  $\Sigma$ , this implies that the highly scattered electrons at these energies are in more nearly “Bloch-like” wave functions in the warm alloy than in the static alloy. The change in  $\Lambda$  has the same general character as in the first case discussed, and here again it shows the tendency towards a spreading of the spectrum. In Fig. 1(c),  $x = 0.1$ ,  $\delta = 1.0$ , the static-alloy band is split. The static alloy is characterized by a virtual crystal  $\Delta$  in the host subband, and a very high  $\Delta$  in the impurity subband strongly peaked near the band gap. As expected from the previous two cases, the thermal disorder increases  $\Delta$  in the virtual-crystal region, but decreases  $\Delta$  at energies of very high damping. Since the static band is already split, the shift of the energy spectrum for each subband causes a stretching of the band.

We would like to emphasize the unusual behavior of  $\Delta$  caused by the thermal disorder when the alloy scattering is strong. We find that the change of  $\Delta$  due to thermal fluctuation of the electronic energy depends on the scattering character of the static alloy. For low static-alloy  $\Delta$ , thermal disorder

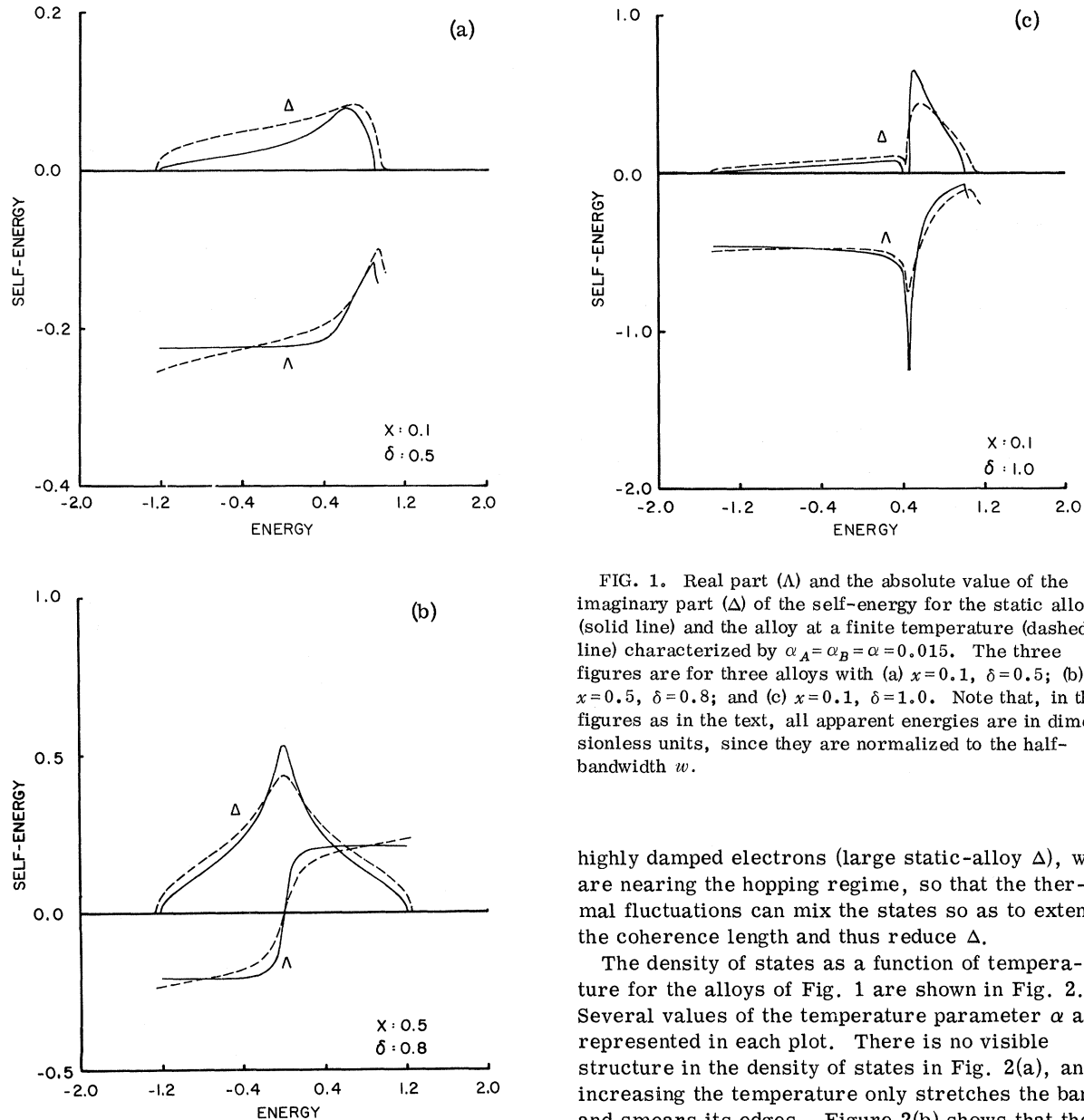


FIG. 1. Real part ( $\Lambda$ ) and the absolute value of the imaginary part ( $\Delta$ ) of the self-energy for the static alloy (solid line) and the alloy at a finite temperature (dashed line) characterized by  $\alpha_A = \alpha_B = \alpha = 0.015$ . The three figures are for three alloys with (a)  $x = 0.1$ ,  $\delta = 0.5$ ; (b)  $x = 0.5$ ,  $\delta = 0.8$ ; and (c)  $x = 0.1$ ,  $\delta = 1.0$ . Note that, in the figures as in the text, all apparent energies are in dimensionless units, since they are normalized to the half-bandwidth  $w$ .

increases the electron damping  $\Delta$  monotonically for all energies. However for the highly impurity damped, short coherence-length states, that might be called "quasilocalized," the thermal disorder actually decreases  $\Delta$ . While no analytical proof has been extracted from the self-consistent integral equation to support our intuitive physical interpretation for the behavior of  $\Delta$ , we speculate as follows. Thermal disorder can do two things to the electrons: It scatters the electrons when they are in more or less "Bloch-like" states, or it can assist the hopping of the highly damped, "quasilocalized" states. Thus, for small static-alloy  $\Delta$ , thermal disorder increases  $\Delta$ . However, for

highly damped electrons (large static-alloy  $\Delta$ ), we are nearing the hopping regime, so that the thermal fluctuations can mix the states so as to extend the coherence length and thus reduce  $\Delta$ .

The density of states as a function of temperature for the alloys of Fig. 1 are shown in Fig. 2. Several values of the temperature parameter  $\alpha$  are represented in each plot. There is no visible structure in the density of states in Fig. 2(a), and increasing the temperature only stretches the band and smears its edges. Figure 2(b) shows that the dip in the static density of states is gradually filled and disappears. The same long band tails appear for big values of  $\alpha$ . In Fig. 2(c), we start with a split static-alloy band. But the band gap is very small, so the thermal fluctuation in the energy can easily close the band gap, and fill it up completely for big  $\alpha$  values.

The electron-phonon interaction, of course, can cause different fluctuations in the scattering strengths for  $A$  atoms and  $B$  atoms, so that  $\alpha_A \neq \alpha_B$ . Figure 3 shows the plots corresponding to those in Figs. 1(b) and 2(b). The only difference is that  $\alpha_A$  is set to be four times as big as  $\alpha_B$ , i. e.,  $\alpha_A/\alpha_B = 4$  and  $\alpha_B = \alpha$ . The effect on the self-energy is a bigger change in both  $\Lambda$  and  $\Delta$  in the upper

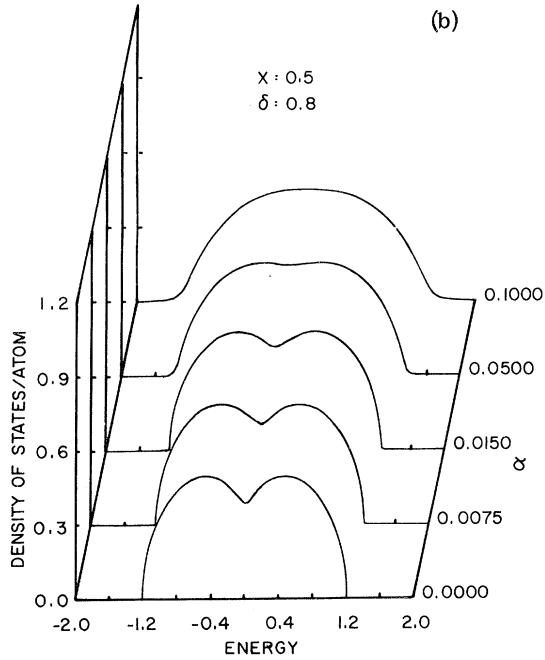
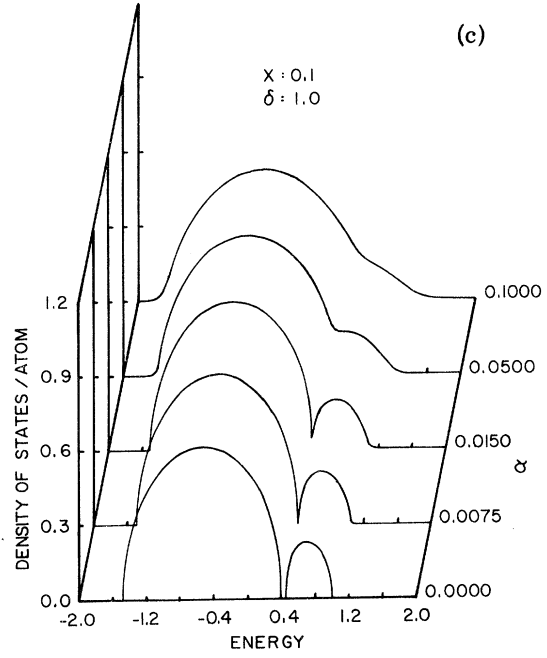
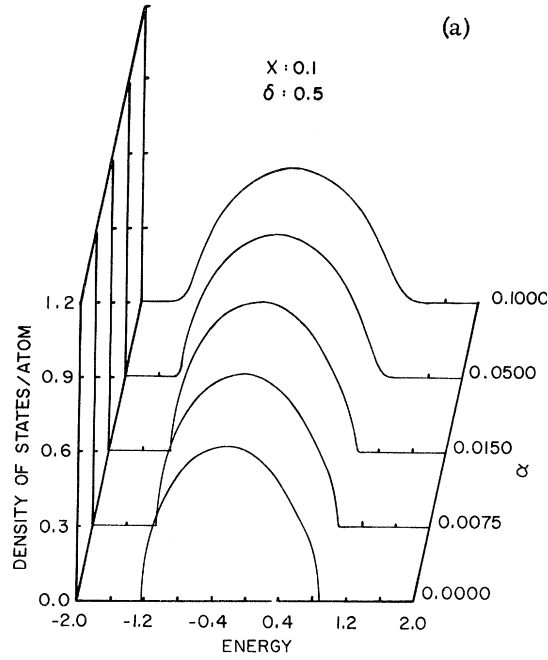


FIG. 2. Density of states ( $E$ ) at five temperatures characterized by  $\alpha=0.0, 0.0075, 0.015, 0.05,$  and  $0.1$ , and  $\alpha_A=\alpha_B=\alpha$ . The three figures are for three alloys with (a)  $x=0.1, \delta=0.5$ ; (b)  $x=0.5, \delta=0.8$ ; and (c)  $x=0.1, \delta=1.0$ . Energies are in dimensionless units.

part of the band, with  $\Sigma$  in the lower part being almost like that in Fig. 1(b). Similarly, the density of states is no longer symmetric, the upper-energy part being stretched more than the lower-energy part.

These results can be better visualized through the study of component densities of states. The self-consistent equation (115) for  $\Sigma$  can be rewritten as a simpler expression for  $F$  by using the equality

in Eq. (116),

$$\begin{aligned} F &= \langle \langle [z - (\mathcal{E}_n + \theta_n) - \frac{1}{4}F]^{-1} \rangle \rangle \\ &= \int d\eta x P_A(\eta) (z - \mathcal{E}_A - \eta - \frac{1}{4}F)^{-1} \\ &\quad + \int d\eta y P_B(\eta) (z - \mathcal{E}_B - \eta - \frac{1}{4}F)^{-1} . \end{aligned} \quad (124)$$

The quantities

$$F_{A,B}(\eta, z) \equiv (z - \mathcal{E}_{A,B} - \eta - \frac{1}{4}F)^{-1} \quad (125)$$

have a special meaning.  $F_A(\eta, z)$  means the site-diagonal matrix element of a restricted-averaged Green function at the site zero. The restriction is that an  $A$  atom is definitely at site zero with a "phonon level shift"  $\eta$ . In the CPñ language,<sup>42</sup> this corresponds to a one-atom cluster, i. e.,  $CP_1(A, \eta)$ . We are simply using the Green function of a crystal characterized by the level  $\mathcal{E}_A + \eta$  at site zero, and by  $\Sigma_{CPA}$  at all other sites, i. e.,

$$\begin{aligned} F_A(\eta, z) &= \langle 0 | [z - H_0 - \hat{\Sigma} - |0\rangle(\mathcal{E}_A + \eta - \Sigma)\langle 0|] | 0 \rangle \\ &= F(z) [1 - (\mathcal{E}_A + \eta - \Sigma)F]^{-1} = (1/F - \mathcal{E}_A - \eta - \Sigma)^{-1} \\ &= (z - \mathcal{E}_A - \eta - \frac{1}{4}F)^{-1} . \end{aligned} \quad (126)$$

If we take the imaginary part of both sides of Eq. (126), and relate  $\text{Im}F$  to the density of states  $\varkappa(E)$  through Eq. (68), we have

$$\varkappa(E) = \int d\eta [xP_A\nu_A(\eta, E) + yP_B(\eta)\nu_B(\eta, E)] , \quad (127)$$

where  $\nu_{A,B}(\eta, E)$  are "local densities of states" and

are defined by

$$\nu_{A,B}(\eta, E) \equiv - (1/\pi) \text{Im}F_{A,B}(\eta, E + i0) . \quad (128)$$

Or, after integration, Eq. (127) may be rewritten, in terms of what will be called "component densities of states," as

$$\varkappa(E) = x\varkappa_A(E) + y\varkappa_B(E) . \quad (129)$$

Thus, the total density of states is the sum of the component densities of states  $\varkappa_A(E)$  and  $\varkappa_B(E)$  weighted by their concentrations. The component density of states  $\varkappa_{A,B}(E)$  at finite temperature differs from the corresponding static-component density of states  $\varkappa_{A,B}^{(0)}(E)$  by a smearing due to thermal fluctuations. The systematic changing of  $\varkappa_{A,B}(E)$  as a function of the temperature parameter  $\alpha$  is shown in Fig. 4.

Note that in one special case, the algebra of our model forces a very simple kind of behavior. In a 50-50 alloy, with  $\alpha_A = \alpha_B$ ,  $\Lambda$  should be antisymmetric and  $\Delta$  symmetric in  $E$ . At the center of the band ( $E=0$ ),  $\varkappa$  and  $\Delta$  will always go oppositely with a change of temperature,  $\varkappa$  increasing when  $\Delta$  decreases, and vice versa. This can be seen from the relation between  $\varkappa$  and  $\Sigma$ ,

$$\varkappa(E) = \frac{1}{\pi} \int d\epsilon \frac{\varkappa_0(\epsilon)\Delta(E)}{(E - \Lambda(E) - \epsilon)^2 + \Delta^2(E)} , \quad (130)$$

which is a combination of Eq. (62), (67), and (68). Since  $\Lambda(0)=0$ ,  $\varkappa(0)$  is a convolution of  $\varkappa_0(0)$  with a Lorentzian centered at  $\epsilon=0$ , and having a width  $\Delta(0)$ . In our model,  $\varkappa_0(\epsilon)$  peaks at  $\epsilon=0$  [see Eq. (102)]. Thus the bigger the width of the Lorentzian, the smaller the convolution will be. So  $\varkappa(0)$  decreases with an increase of  $\Delta(0)$ . For any symmetric, centrally peaked  $\varkappa_0(0)$ , i. e.,  $\varkappa_0(\epsilon) = \varkappa_0(-\epsilon)$  and  $\varkappa_{0\text{max}} = \varkappa_0(0)$ , we can draw the same conclusion.

Note also that the change in the damping of the electron states caused by the thermal disorder, and therefore the criterion for the sign of that change, can be determined by a perturbation solution to the self-consistent equation for  $F$  (see Appendix D). However, the criterion is in terms of  $F^{(0)}$ , which is only an implicit function [Eq. (117)] of the input parameters  $x$  and  $\delta$ . A study of the criterion in terms of the input parameters is rather tedious. However, in the simple case where  $x=0.5$ ,  $\alpha_A = \alpha_B$ , and the energy is at the center of the band ( $E=0$ ), it turns out (see Appendix G) that  $(\partial\Delta/\partial\alpha)|_{E=0}$  is positive when  $\delta < \frac{1}{2}$ , and negative when  $\frac{1}{2} < \delta < 1$ . (Notice that when  $\delta > 1$ , the band is split.) This fits our speculation about the effect of the thermal fluctuations on  $\Delta$ .

Turning to the conductivity, once the density of states and the imaginary part of the self-energy are known, the conductivity as a function of the

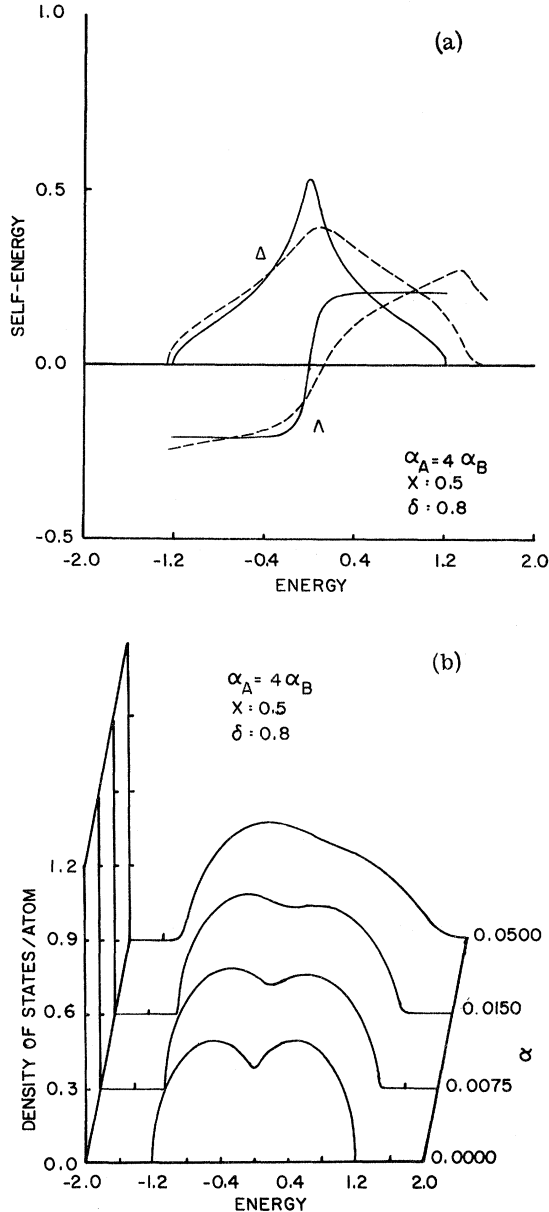


FIG. 3. (a) Self-energy for the alloy with  $x=0.5$ ,  $\delta=0.8$ , and  $\alpha_A=4\alpha_B=4\alpha$  at two temperatures characterized by  $\alpha=0.0$  (solid line) and  $\alpha=0.015$  (dashed line). (b) The density of states for the same alloy at four temperatures characterized by  $\alpha=0.0, 0.0075, 0.015$ , and  $0.05$ . Energies are in dimensionless units.

Fermi level is easily obtained from Eq. (112). Figures 5(a)–(c) are the corresponding conductivity for alloys with the same parameters as shown in Figs. 2(a)–(c), while Fig. 5(d) is the one corre-

sponding to Fig. 3(b). In the virtual crystal [i. e., Figs. 2(a) and 5(a)], the change in the density of states for small  $\alpha$  is not visible, but the change in the conductivity is very big. Thus, in this case the

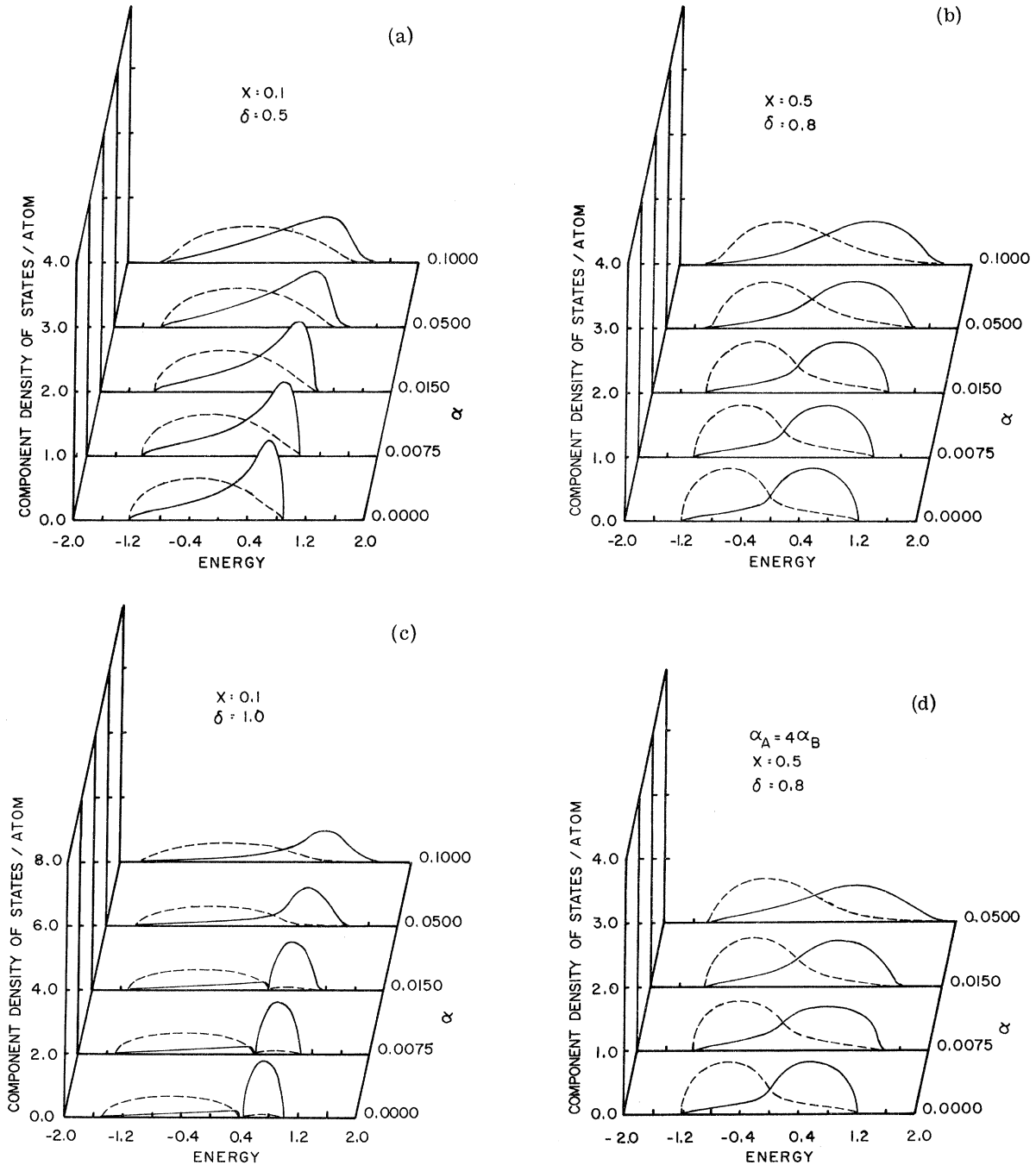


FIG. 4. Component densities of states,  $\mathcal{N}_A$  (solid line) and  $\mathcal{N}_B$  (dashed line), as defined in Eqs. (127) and (129) at several temperatures characterized by different  $\alpha$  values. The four figures are for alloys with (a)  $x=0.1$ ,  $\delta=0.5$ ,  $\alpha_A=\alpha_B=\alpha$ ; (b)  $x=0.5$ ,  $\delta=0.8$ ,  $\alpha_A=\alpha_B=\alpha$ ; (c)  $x=0.1$ ,  $\delta=1.0$ ,  $\alpha_A=\alpha$ ; and (d)  $x=0.5$ ,  $\delta=0.8$ , but  $\alpha_A=4\alpha_B=4\alpha$ . Energies are in dimensionless units.



electron-phonon interaction is the dominant mechanism for the resistivity at high temperatures. On the other hand, in the alloy with a high "impurity resistivity" [Figs. 2(b) and 5(b)], the relative change

in the conductivity is not very large. In the split-band limit, when the Fermi level is at the band edge or in the band gap, the degenerate Fermi statistics leads to the zero conductivity that may

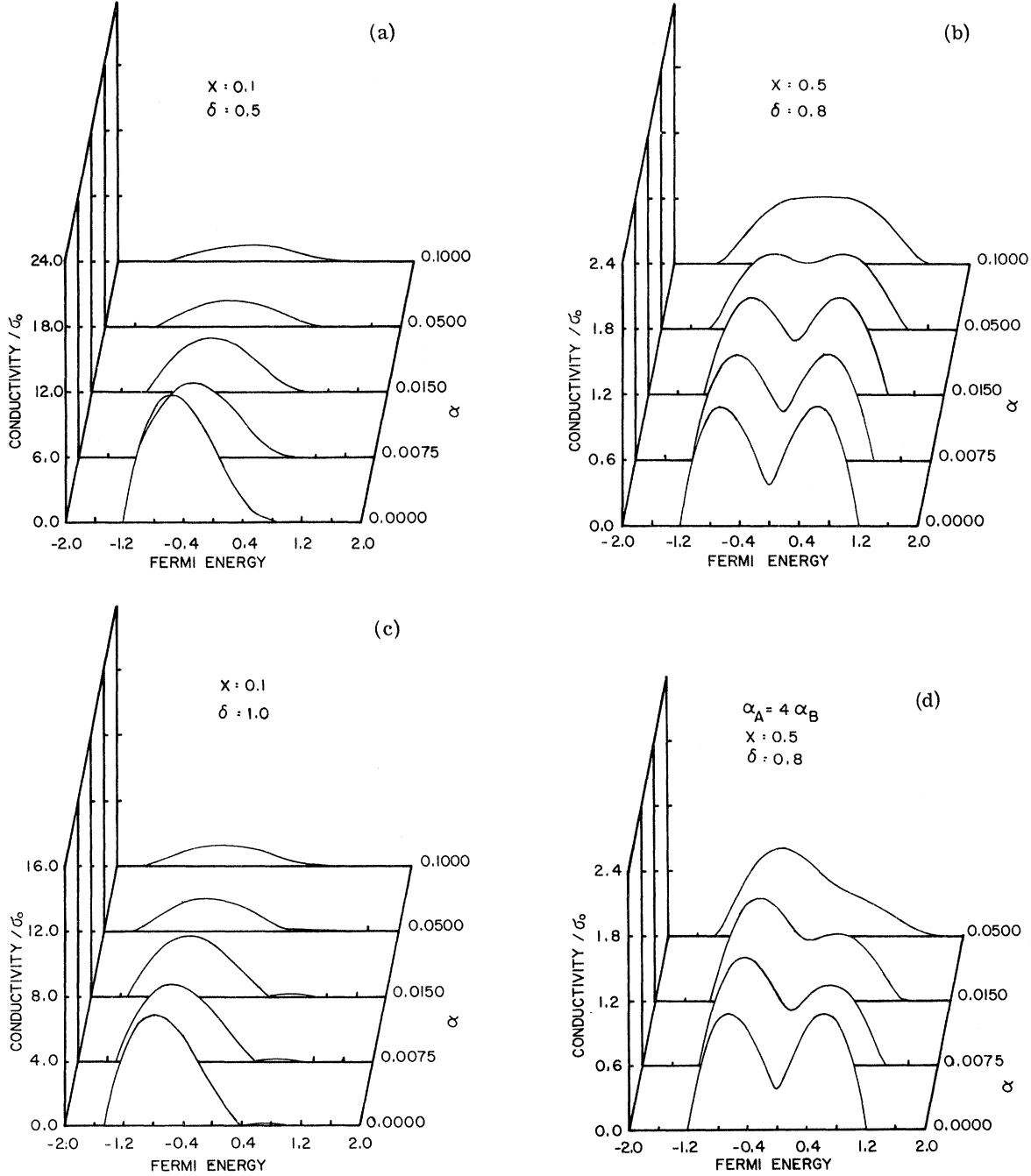


FIG. 5. Electrical conductivity  $\sigma$  calculated from Eq. (112) as a function of the Fermi energy at different  $\alpha$  values. The four figures are alloys with (a)  $x=0.1$ ,  $\delta=0.5$ ,  $\alpha_A=\alpha_B=\alpha$ ; (b)  $x=0.5$ ,  $\delta=0.8$ ,  $\alpha_A=\alpha_B=\alpha$ ; (c)  $x=0.1$ ,  $\delta=1.0$ ,  $\alpha_A=\alpha_B=\alpha$ ; and (d)  $x=0.5$ ,  $\delta=0.8$ ,  $\alpha_A=4\alpha_B=4\alpha$ . Note that, here and in the rest of the figures,  $\sigma_0$  is equal to  $\pi^2 e^2 \hbar v_m^2 / 12 \Omega_c$ . Energies are in dimensionless units.

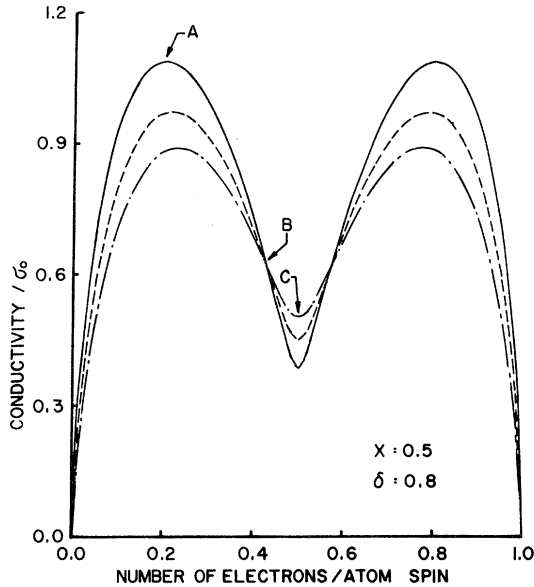


FIG. 6. Electrical conductivity as a function of the numbers of electrons per atom per spin for the alloy with  $x=0.5$ ,  $\delta=0.8$ ,  $\alpha_A=\alpha_B=\alpha$ . The three curves represent the static alloy (—) and the alloys with  $\alpha=0.0075$  (---) and  $\alpha=0.015$  (-·-·-). Arrows indicate three different temperature resistivity coefficients of electrical resistivity. At A,  $d\rho/dT$  is positive; at B, zero; at C, negative.

be observed in the static-alloy curve. When thermal disorder is introduced, the band gaps are filled so that the conductivity becomes nonzero. However, we cannot rely on CPA to describe the "impurity-band" conductivity, since the cluster effect is very important in this case.<sup>57</sup>

In practice, the conductivity of an alloy is investigated as a function of temperature by fixing the average number of electrons per atom,  $C$  [see Eq. (122)], instead of fixing the Fermi level. Although it is difficult to experimentally adjust  $C$ , it is convenient and instructive to plot the conductivity as a function of  $C$ . In Fig. 6 we study this kind of plot for the case  $x=0.5$ ,  $\delta=0.8$ . The solid line represents the static alloy; the other two dashed lines are the alloy with  $\alpha=0.0075$  and  $0.015$ , respectively. It is interesting to see that the conductivity can either increase or decrease with temperature depending on the number of electrons per atom for the alloy. In other words, the temperature coefficients of conductivity are very sensitive to the location of the Fermi level. For the same band structure, the three different locations of Fermi energy, as shown by the arrows, give three qualitatively different results for  $d\rho/dT$ : At A it is positive; at B, zero; at C, negative. The corresponding resistivity-vs-temperature curves for these three cases are shown in Fig. 7. This kind of behavior of the conductivity

depends on the strong-scattering character of the static alloy. In contrast, Fig. 8 shows that nothing unusual happens for a weak-scattering (small  $\delta$ ) alloy, even though it is concentrated. The conductivity, here decreases monotonically with increasing temperature for any Fermi energy. Finally, let us investigate the influence of different  $\alpha_A$  and  $\alpha_B$  on the temperature variation of the conductivity. The input parameters for Fig. 9 differ from those of Fig. 6 only in that in Fig. 9  $\alpha_A$  is four times as big as  $\alpha_B$  (in both figures  $\alpha_B=\alpha$ ). The conductivity is no longer symmetrical with respect to the center, the electron conductivity being bigger than the hole conductivity at finite temperatures.

#### F. Implications of Model Calculation

We have presented the main features of the model calculation. The most obvious conclusion that may be drawn from our data can be put in this way: The thermal disorder broadens and smears the electronic density of states in the alloy. It raises the electrical resistivity in the virtual-crystal limit, but, in a strong-scattering alloy, produces an increase or decrease in conductivity depending on the location of the Fermi energy. We can say more, which is outlined as follows. Since we have treated the density of states and conductivity adequately in a model which has many of the characteristics of an alloy, we should look for any physical ideas that might be suggested by our experience with the model. Along these lines, we

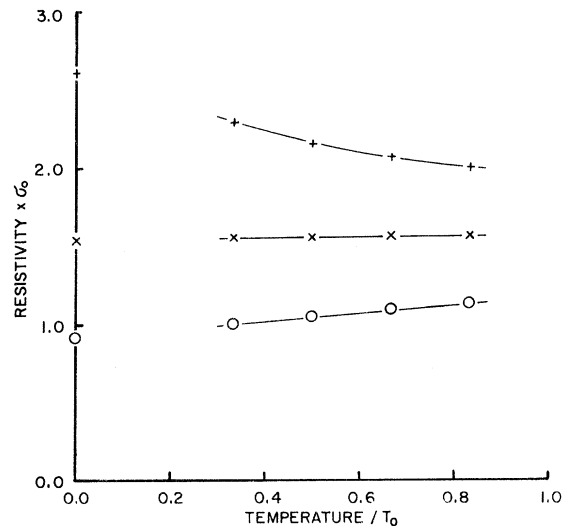


FIG. 7. Electrical resistivity as a function of temperature corresponding to the three cases indicated by the arrows in Fig. 6. Here  $\circ$  is for case A,  $\times$  for case B, and  $+$  for case C. Here  $T_0$  is the temperature such that  $\alpha(T_0)$  is  $0.018$ , and  $\alpha$  is approximated to be linear with temperature (see Appendix A).

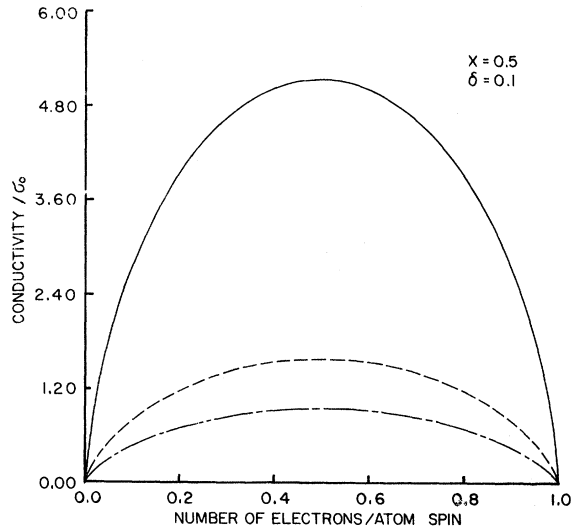


FIG. 8. Electrical conductivity as a function of the number of electrons per atom per spin for the alloy with  $x=0.5$ ,  $\delta=0.1$ ,  $\alpha_A=\alpha_B=\alpha$ . The three curves represent the static alloy (—) and the alloys with  $\alpha=0.006$  (---) and  $\alpha=0.012$  (-·-·-).

will first ask what help perturbation theory can give us. Then, we compare the elementary expression for conductivity with the CPA formula, both generally and in a limiting case. In the process, we discover a need to reexamine the meaning of the self-energy. Finally, the complications inherent in real transition-metal alloys are considered.

In a concentrated, strong-scattering alloy, the electron-phonon interaction is small compared to the "impurity" scattering, but it is the essential mechanism governing the temperature dependence. (In our case it is the only mechanism.) It is believed that the lowest-order contribution of the electron-phonon interaction to the resistivity, calculated by the usual perturbation theory, should give the correct answer. In our case this technique is prohibited by our poor knowledge of the nature of the static alloy. For example, let us expand the Green function  $G$  [Eq. (18)] in terms of the static-alloy Green function  $G_s$ ,

$$G = G_s + G_s \Theta G_s + G_s \Theta G_s \Theta G_s + \dots, \quad (131)$$

where  $G_s$  is defined as [see Eq. (52)]

$$G_s \equiv (z - H_0 - D)^{-1}. \quad (132)$$

When we average on both sides on Eq. (131), we get

$$\langle\langle G \rangle\rangle = \langle G_s \rangle_c + \langle G_s \Theta G_s \Theta \rangle_p G_s \rangle_c + \dots. \quad (133)$$

To use perturbation theory based on the static alloy, we need to know the three-Green-function average  $\langle G_s \Theta G_s \Theta \rangle_p G_s \rangle_c$  very well, which is an unsolved problem to date. Therefore, we use the alternate method of the self-consistent CPA equations.

The Kubo-Greenwood formula for electrical conductivity in CPA and our model has been reduced to the very simple and explicit expression, Eq. (112), which is only a function of the density of states  $\mathcal{N}$  and the absolute value of the imaginary part of the self-energy  $\Delta$  at the Fermi energy. Notice that, for a free-electron band with concentrated scatters, we get Eq. (112) without the  $6\Delta/\pi\mathcal{N}$  correction term (see Appendix E). The form of Eq. (112) makes for easy comparison with the elementary formula for resistivity,<sup>58</sup>

$$\rho = \frac{3}{e^2 v_F^2} \frac{1}{D(\epsilon_F)} \frac{1}{\tau}, \quad (134)$$

where  $D(\epsilon_F)$  is the density of states per unit volume at the Fermi energy (including both spins),  $\tau$  is the collision time, and  $v_F$ , the velocity of the electron at  $\epsilon_F$ . The comparison should be meaningful only near the low-collision-rate regime, where Eq. (134) is accurate. We can identify

$$D(\epsilon_F) = (2/\Omega_c) \mathcal{N}(\epsilon_F), \quad (135)$$

and force

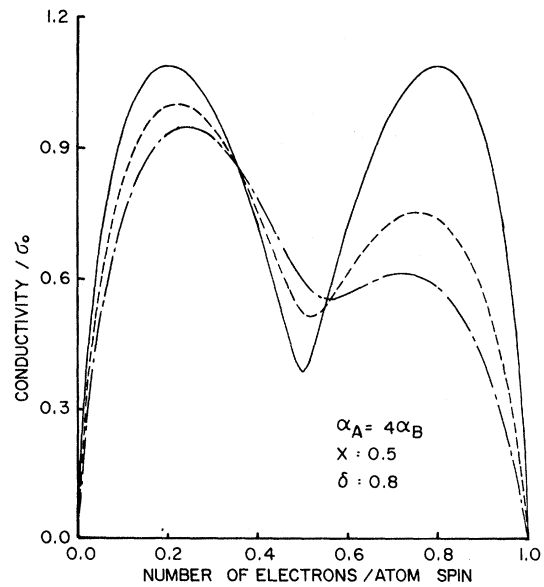


FIG. 9. Conductivity as a function of electrons per atom per spin for the alloy with  $x=0.5$ ,  $\delta=0.8$ , and  $\alpha_A=4\alpha_B=4\alpha$ . The three lines are for three temperatures characterized by  $\alpha=0.0$  (—),  $\alpha=0.0075$  (---), and  $\alpha=0.015$  (-·-·-).

$$v_F^2 \tau = \frac{\pi^2 v_m^2 \mathcal{V}^2(\epsilon_F)}{4} \left( 1 + \frac{6\Delta}{\pi \mathcal{V}} \right) \left( \frac{\hbar}{2\Delta} \right) . \quad (136)$$

How are we to identify  $v_F^2$  and  $\tau$  on the right-hand side of the equation? Can  $\tau$  be identified with  $\hbar/2\Delta$ ? This is a temptation that we shall show is fully justified only for low scattering rates. We need to understand the physical meaning of  $\Delta(\epsilon_F)$  or the whole self-energy  $\Sigma$  in order to answer these questions.

The basic definition of the self-energy is Eq. (28). We get a better feeling for  $\Sigma$  if we think of  $\langle\langle G(z) \rangle\rangle$  as a propagator, and use the relation between the ensemble-averaged time evolution operator  $\langle\langle U(t) \rangle\rangle$  and  $\langle\langle G(z) \rangle\rangle$ ,

$$\langle\langle U(t) \rangle\rangle = (-1/2\pi i) \oint dz e^{-izt} \langle\langle G(z) \rangle\rangle . \quad (137)$$

The clockwise contour includes the real axis and surrounds the lower half  $z$  plane. Consider how an eigenstate of  $H_0$ , say a "mock Bloch state"  $|\vec{k}\rangle$  in our case, evolves. Since  $\hat{\Sigma}$  is diagonal in  $|\vec{k}\rangle$ , the probability amplitude for finding a state surviving after a time  $t$  is

$$\begin{aligned} \alpha_{\vec{k}}(t) &= \langle \vec{k} | \langle\langle U(t) \rangle\rangle | \vec{k} \rangle \\ &= (-1/2\pi i) \oint dz e^{-izt} \langle \vec{k} | (z - H_0 - \hat{\Sigma})^{-1} | \vec{k} \rangle \\ &= (-1/2\pi i) \oint dz e^{-izt} [z - \epsilon(\vec{k}) - \Sigma(z, \vec{k})]^{-1} \\ &= (-1/2\pi i) \oint dz e^{-izt} g(\vec{k}, z) . \end{aligned} \quad (138)$$

Or, after integration,

$$\alpha_{\vec{k}}(t) = e^{-iz_1(\vec{k})t} , \quad (139)$$

where  $z_1(\vec{k})$  is the pole of  $g(\vec{k}, z)$  inside the contour. Thus, the real part of  $z_1$  is the shifted spectrum corresponding to  $\epsilon(\vec{k})$ , and the imaginary part of  $z_1$  measures the ensemble-averaged decay of the "Bloch" states  $|\vec{k}\rangle$ . The decay time of the  $|\vec{k}\rangle$  state is

$$\tau_{\vec{k}} = \hbar/2[-\text{Im}z_1(\vec{k})] . \quad (140)$$

But the location of the pole at  $z_1$  and the self-energy  $\Sigma(z_1)$  are closely related by

$$\text{Re}z_1(\vec{k}) = \epsilon(\vec{k}) + \text{Re}\Sigma(z_1, \vec{k}) , \quad (141)$$

and

$$\text{Im}z_1(\vec{k}) = \text{Im}\Sigma(z_1, \vec{k}) . \quad (142)$$

Therefore, the self-energy at the poles of  $g(\vec{k}, z)$  has a very simple physical meaning: The real part of  $\Sigma$  is the shift of the energy level  $\epsilon(\vec{k})$  in the alloy, the imaginary part is the uncertainty of this energy level in the ensemble.

However, the self-energies in the formulas for the density of states and conductivity [see Eqs. (20), (22), (23), and (24)] are at the energies  $z = E \pm i0$ . These are not necessarily the poles of  $g(\vec{k}, z)$ . Thus, we have a physical interpretation for  $\Sigma(z_1)$ , but what we need is the meaning of  $\Sigma(E \pm i0)$ .

Suppose we construct states  $|\psi_{\nu E}\rangle$  with a sharp energy  $E$  in a particular alloy and phonon configuration, and this state has the expression

$$|\psi_{\nu E}\rangle = \sum_{\vec{k}} A_{\nu}(E, \vec{k}) |\vec{k}\rangle . \quad (143)$$

Then the average energy-momentum density of states, i. e., the spectral function, is

$$\begin{aligned} &\left\langle\left\langle \sum_{\nu E'} |A_{\nu}(E', \vec{k})|^2 \delta(E - E') \right\rangle\right\rangle \\ &= \frac{1}{\pi} \frac{\Delta(E, \vec{k})}{[E - \epsilon(\vec{k}) - \Lambda(E, \vec{k})]^2 + \Delta^2(E, \vec{k})} , \end{aligned} \quad (144)$$

as is well known from elementary Green-function theory. In our case, the self-energy is independent of  $\vec{k}$ , so we have

$$\begin{aligned} &\left\langle\left\langle \sum_{\nu E'} |A_{\nu}(E', \vec{k})|^2 \delta(E - E') \right\rangle\right\rangle \\ &= \frac{1}{\pi} \frac{\Delta(E)}{[E - \epsilon(\vec{k}) - \Lambda(E)]^2 + \Delta^2(E)} . \end{aligned} \quad (145)$$

Thus, if we take Eq. (145) as giving us the spectral density of a typical exact energy state of the alloy, then  $\Delta(E)$  gives us a spectral width in terms of the pure perfect crystal spectrum  $\epsilon(\vec{k})$ . In other words, the alloy energy state is composed of "Bloch" states ranging over  $\vec{k}$ , with a spread  $\Delta(E)$ , in  $\epsilon(\vec{k})$ , so that the lifetime of coherence of the alloy wave function, when it is in a pure perfect crystal, is

$$\tau_c = \hbar/2\Delta(E) . \quad (146)$$

Thus, our conductivity formula does not manifestly contain the usual collision time of a Bloch state. However, in the virtual-crystal limit there is not much difference between these two relaxation times. The CPA result for the self-energy in this limit is (see Appendix C)

$$\Sigma(z) \simeq \bar{\epsilon} + (xy\delta^2 + x\alpha_A + y\alpha_B)F_0(z - \Sigma) . \quad (147)$$

In order to find the pole of  $g(\vec{k}, z)$ , we need  $z_1 - \Sigma = \epsilon(k)$ , so that Eq. (147) becomes

$$z_1 - \epsilon(\vec{k}) \simeq \bar{\epsilon} + (xy\delta^2 + x\alpha_A + y\alpha_B)F_0(\epsilon(\vec{k}) + i0) , \quad (148)$$

where we have set  $\epsilon(\vec{k})$  to  $\epsilon(\vec{k}) + i0$  in order to have a negative imaginary part for  $z_1$ . Using Eq. (140), we have

$$\frac{1}{\tau_{\vec{k}}} = \frac{2\pi}{\hbar} (xy\delta^2 + x\alpha_A + y\alpha_B)\mathcal{V}_0(\epsilon(\vec{k})) . \quad (149)$$

On the other hand, if we find the self-energy at  $\bar{\epsilon} + \epsilon(\vec{k}) + i0$ , we have

$$\Sigma(\bar{\epsilon} + \epsilon(\vec{k}) + i0) \approx \bar{\epsilon} + (xy\delta^2 + x\alpha_A + y\alpha_B)F_0(\epsilon(\vec{k}) + i0) , \quad (150)$$

so that

$$\Delta(\bar{\epsilon} + \epsilon(\vec{k})) = (xy\delta^2 + x\alpha_A + y\alpha_B) \pi \mathfrak{N}_0(\epsilon(\vec{k})) . \quad (151)$$

The collision rate corresponding to the coherence time  $\tau_c$  is

$$\begin{aligned} \frac{1}{\tau_c(\bar{\epsilon} + \epsilon(\vec{k}))} &= \frac{2\Delta(\bar{\epsilon} + \epsilon(\vec{k}))}{\hbar} \\ &= \frac{2\pi}{\hbar} (xy\delta^2 + x\alpha_A + y\alpha_B) \mathfrak{N}_0(\epsilon(\vec{k})) , \end{aligned} \quad (152)$$

which is identical with  $1/\tau_{\vec{k}}$  in Eq. (149).

Now that we have examined the relation between  $\Delta$  and the collision time, we shall consider the  $v_F^2$  factor. The average of the squared velocity taken over all states at the Fermi energy  $\epsilon_F$  may be calculated in CPA and within our model (see Appendix F) with the result,

$$\begin{aligned} \langle\langle v_F^2 \rangle\rangle &= \text{Tr} \langle\langle (\vec{p}/m)^2 \delta(\epsilon_F - H) \rangle\rangle [\text{Tr} \langle\langle \delta(\epsilon_F - H) \rangle\rangle]^{-1} \\ &= v_m^2 \left[ \frac{\pi^2 N^2}{4} + \frac{3\Delta}{\pi N} \left( 1 + \frac{4\Delta}{\pi \mathfrak{N}} \right)^{-1} \right] . \end{aligned} \quad (153)$$

When we substitute the values for  $\mathfrak{N}$  and  $\Delta$  for the 50-50-static-alloy case, with the Fermi energy at the center of the band,  $\epsilon_F = 0$ , we find (see Appendix G),

$$\langle\langle v_F^2 \rangle\rangle = v_m^2 (1 - \frac{1}{4} \delta^2) . \quad (154)$$

This has the correct value  $v_m^2$  at  $\delta = 0$  and decreases with increasing  $\delta$ , as it should.

Remember that in CPA and our model the vertex correction for the current vanishes [see Eq. (73)]. In the weak-scattering limit, the vanishing of the net backward scattering, and, the current relaxation time in the Boltzmann equation equals the single-particle collision time.<sup>9</sup> Thus, for an isotropic band we can obtain the resistivity, correct to order  $\delta^2$  and  $\alpha$ , by assigning a collision time  $\tau_F$  at the Fermi energy  $\epsilon_F = \epsilon(\vec{k}) + \bar{\epsilon}$  as in Eq. (149) or (152), and a Fermi velocity  $v_F^2$  by dropping the correction term in Eq. (153) (see Appendix C), i. e.,

$$\begin{aligned} v_F^2 &\approx \frac{1}{4} \pi^2 v_m^2 \mathfrak{N}_0^2(\epsilon_F - \bar{\epsilon}) \\ &= v^2(\epsilon(\vec{k})) \Big|_{\epsilon(\vec{k}) = \epsilon_F - \bar{\epsilon}} . \end{aligned} \quad (155)$$

Also, in the weak-scattering limit, we can drop the second term in Eq. (112) for the conductivity. Then the CPA results reduce to the elementary formula Eq. (134). However, for a concentrated, strong-scattering alloy, when perturbation theory and the Boltzmann equation are not valid, the contributing factors to the elementary conductivity formula, as well as the formula itself, tend to lose their simple meaning. As should have been expected, the elementary formula, Eq. (134), is lost alto-

gether in the general case. Indeed, the substantial increase of the conductivity with temperature, as in Fig. 5(b) for a half-filled band, is reminiscent of activated-hopping-type conductivity, rather than the free conduction implied in Eq. (134). This thought is in harmony with the tendency toward wave-function localization that is reflected in the high values of the static-alloy  $\Delta$  (and  $\Delta/\mathfrak{N}$ ) found in the same cases. This tendency to localization seems to be reduced there, by the thermal disorder. Note, however, that CPA is not reliable near band edges, a situation that we may begin to approach in Fig. 5(b) near  $\epsilon_F = 0$ , i. e., near the top of the bottom band and the bottom of the top band. Although we cannot trust the exact calculated magnitudes, we believe that the CPA result indicates a real trend.

A word is in order here on the difficulties and complications that still separate a calculation like the present one from a realistic treatment of the transition-metal alloys. In the first place, these metals have a complicated band structure.<sup>59</sup> At least six bands are involved, instead of one, none of the bands<sup>60</sup> having a true tight-binding character, and most of the bands (the  $d$  bands) being extremely sensitive to small changes in the potential,<sup>61</sup> or crystal structure. This sensitivity implies that the self-consistent-field (SCF) potential may be hard to take into account, the potential at one atomic cell being dependent on the configuration in its neighborhood, the electronic structure dependent on the potential, the electronic density on electronic structure, the potential on the electronic density, and so on, in a vicious circle. The change in band structure with temperature, due to expansion and other effects, may be difficult and important. In addition, not all configurations are equally likely, but rather there is some correlational clustering of atoms<sup>62</sup> at best, and defects could be important in transition-metal alloys made with a minimum of correlational clustering. Then, one may be extremely near a significant band edge, as in constantan,<sup>63</sup> and generally transition-metal conduction bands are jungles of singularities. Under such conditions, cluster effects are very important and CPA inadequate, as we have mentioned earlier. The electron-phonon interaction, also, is nontrivial in the transition metals, and all the more so in the alloys. Even the phonon spectrum itself changes significantly with alloying.<sup>64</sup> One of the most serious problems, along with the band-structure complications mentioned above, is that all of the transition metals tend to have various magnetic properties. There are giant "polarization clouds" in at least some carefully made Cu-Ni alloys,<sup>62,65</sup> and a Kondo-like resistivity-minimum-type effect<sup>66</sup> is probably extremely important, and should be explored in a semiempirical way separately from

all the other influence that we have mentioned. One element of simplicity in the problem is that in Ni-Cu alloys, the "s electrons" apparently carry most of the current. This idea, which has been present in the literature for many years on the basis of a vague hypothetical picture<sup>28</sup> of the transition-metal band structure, turns out to be accurate<sup>67</sup> for Cu-Ni (but probably not in some other transition-metal alloys) as a result of an involved numerical balance among several competing effects. A hopeful sign is that some theoretical results based on fairly realistic atomic potentials should be available in the near future.<sup>68</sup> We have a long way to go, but some of the basic questions are now within reach.

#### ACKNOWLEDGMENT

We wish to thank C. Gross who initially stimulated our interest in this problem, and has on several occasions informed us of his experimental results prior to publication.

#### APPENDIX A: ROUGH ESTIMATES OF THERMAL FLUCTUATION PARAMETER $\alpha$ AT HIGH TEMPERATURES

##### 1. Nearly-Free-Electron Case

In a nearly-free-electron model, an approximation to the fluctuation of the electron energy caused by lattice vibrations can be found from deformation-potential theory.<sup>69</sup> The energy fluctuations  $\delta\mathcal{E}$  are mainly due to the charge shift needed to keep a constant chemical potential throughout the crystal when the crystal is distorted by a phonon<sup>70</sup>:

$$\delta\mathcal{E} \approx -\frac{2}{3} \mathcal{E}_F \mathcal{D} \quad , \quad (\text{A1})$$

where  $\mathcal{D}$  is the dilatation. Then  $\alpha$  is just the mean square of the energy fluctuation

$$\alpha = \langle \delta\mathcal{E}^2 \rangle_p \approx \frac{4}{9} \mathcal{E}_F^2 \langle \mathcal{D}^2 \rangle_p \quad . \quad (\text{A2})$$

The mean square of the dilatation can be related to the melting point by using the Lindemann melting criterion, with the result<sup>71</sup>

$$\langle \mathcal{D} \rangle_p \approx 0.04 T/T_m \quad ,$$

where  $T$  is the absolute temperature and  $T_m$  is the melting point. If the Fermi level is at the center of the band, then  $\mathcal{E}_F = 1$  in units of half-bandwidth, and we have

$$\alpha \approx 0.02 T/T_m \quad . \quad (\text{A3})$$

##### 2. Typical $d$ Band in Noble and Transition Metals

The  $d$  bands have too much structure to be represented well by a semiellipse density of states curve. Therefore, our rough estimate must be made carefully. For alloys with a nearly full  $d$  band, e.g., Ni-Cu, we may focus our attention on the topmost  $d$ -band region or "subband," which has a marked peak in the density of states.

If we identify the root-mean-square energy fluctuation of the relevant  $d$  subband with the typical shift of the  $d$ -band edge,  $\Delta E_s$ , then

$$\alpha \approx (\Delta E_s)^2 \quad . \quad (\text{A4})$$

The typical edge shift is just one-half of the root-mean-square broadening of the bandwidth,  $\delta W_d$ , i. e.,

$$\Delta E_s \approx \frac{1}{2} \delta W_d \quad . \quad (\text{A5})$$

Since the  $d$  bandwidth  $W_d$  is proportional<sup>72</sup> to  $R^{-5}$ , where  $R$  is the lattice constant, we can roughly estimate the root-mean-square change of the width,  $\delta W_d$ , by estimating the root-mean-square change of the radius of an atomic cell  $\delta R$ ,

$$\delta W_d \approx 5(\delta R/R)W_d \quad , \quad (\text{A6})$$

with

$$\delta R = (N_n)^{-1/2} \delta R_{\text{typ}} \quad , \quad (\text{A7})$$

where  $N_n$  is the coordination number of the lattice and  $\delta R_{\text{typ}}$  is the typical root-mean-square atomic displacement.  $\delta R_{\text{typ}}$  can be related to the dilatation  $\mathcal{D}$  by

$$\delta R_{\text{typ}} \approx \frac{1}{3} R [\langle \mathcal{D}^2 \rangle_p]^{1/2} \approx \frac{1}{3} R (0.04 T/T_m)^{1/2} \quad . \quad (\text{A8})$$

Combining Eqs. (A4)–(A8), we find

$$\alpha \approx \frac{25}{36} \frac{W_d^2}{N_n} 0.04 \frac{T}{T_m} \approx 0.03 \frac{W_d^2}{N_n} \frac{T}{T_m} \quad . \quad (\text{A9})$$

In a fcc crystal  $N_n = 12$ , and  $\alpha$  is

$$\alpha \approx 0.003 W_d^2 T/T_m \quad . \quad (\text{A10})$$

For a Ni-Cu alloy, the whole  $d$  bandwidth  $W_d$  is approximately 0.4 Ry. The effective width for the top "subband" is taken to be 0.15 Ry, so that our energy unit is 0.075 Ry. Therefore, an estimate for  $\alpha$  is

$$\alpha \approx 0.003 \left( \frac{0.4}{0.075} \right)^2 \frac{T}{T_m} \approx 0.075 \frac{T}{T_m} \quad . \quad (\text{A11})$$

#### APPENDIX B: EVALUATION OF $\mathcal{L}(\eta)$

The quantity  $\mathcal{L}(\eta)$  is defined in Eq. (109) as

$$\mathcal{L}(\eta) = \int_{-1}^1 d\xi \frac{\Delta^2(\eta)(1-\xi^2)^{3/2}}{\{[\eta - \Lambda(\eta) - \xi]^2 + \Delta^2(\eta)\}^2} \quad , \quad (\text{B1})$$

where  $\Lambda$ ,  $\Delta$  are defined as the real and imaginary parts of the self-energy

$$\Sigma(\eta \pm i0) \equiv \Lambda(\eta) \mp i\Delta(\eta) \quad . \quad (\text{B2})$$

It is convenient to define an auxiliary complex function

$$\begin{aligned} \Phi(z) &= \int_{-1}^1 d\xi \frac{(1-\xi^2)^{3/2}}{z-\xi} \\ &= (1-z^2) \int_{-1}^1 d\xi \frac{(1-\xi^2)^{1/2}}{z-\xi} \end{aligned}$$

$$+ \int_{-1}^1 d\xi (z + \xi)(1 - \xi^2)^{1/2} . \quad (\text{B3})$$

Then in terms of  $\Phi$ ,  $\mathcal{L}(\eta)$  may be rewritten as

$$\begin{aligned} \mathcal{L}(\eta) &= \frac{\Delta}{2} \frac{\partial}{\partial \Delta} \left( \frac{1}{\Delta} \text{Im} \Phi(\eta + i - \Sigma(\eta^*)) \right) \\ &= -\frac{1}{2\Delta} \text{Im}[\Phi(\eta + i0 - \Sigma)] + \frac{1}{2} \text{Im} \left( \frac{\partial}{\partial \Delta} \Phi(\eta + i0 - \Sigma) \right) . \end{aligned} \quad (\text{B4})$$

Using Eqs. (62) and (102), Eq. (B3) may be rewritten as

$$\begin{aligned} \Phi(z) &= \frac{1}{2} \pi (1 - z^2) \int_{-1}^1 d\xi \frac{\mathfrak{X}_0(\xi)}{z - \xi} + \frac{1}{2} \pi z \int_{-1}^1 d\xi \mathfrak{X}_0(\xi) \\ &= \frac{1}{2} \pi [(1 - z^2) F_0(z) + z] . \end{aligned} \quad (\text{B5})$$

There is no contribution to  $\mathcal{L}(\eta)$  from the  $\frac{1}{2} \pi z$  term in  $\Phi$ , since

$$-\frac{1}{\Delta} \text{Im}(\eta + i0 - \Sigma) + \frac{\partial}{\partial \Delta} \text{Im}(\eta + i0 - \Sigma) = 0 .$$

If we define still another function,

$$\psi(z) \equiv (1 - z^2) F_0(z) , \quad z = \eta + i0 - \Sigma(\eta^*) , \quad (\text{B6})$$

then, from Eq. (67),  $\psi(z)$  can also be expressed as

$$\psi(z) = (1 - z^2) F(\eta + i0) . \quad (\text{B7})$$

Then in terms of  $\psi(z)$ ,  $\mathcal{L}(\eta)$  becomes

$$\mathcal{L}(\eta) = \frac{\pi}{4} \left( -\frac{1}{\Delta} \text{Im} \psi(z) + \frac{\partial}{\partial \Delta} \text{Im} \psi(z) \right) . \quad (\text{B8})$$

Next evaluate  $\text{Im} \psi(z)$ ,

$$\begin{aligned} \text{Im} \psi(z) &= -\pi \mathfrak{X}(\eta) - (\text{Re} z^2) [-\pi \mathfrak{X}(\eta)] - (\text{Im} z^2) (\text{Re} F) \\ &= -\pi \mathfrak{X} - [(\eta - \Lambda)^2 - \Delta^2] (-\pi \mathfrak{X}) - 2\Delta(\eta - \Lambda) (\text{Re} F) \\ &= -\pi \mathfrak{X} [1 - (\eta - \Lambda)^2 + \Delta^2 + (2\Delta/\pi \mathfrak{X})(\eta - \Lambda) \text{Re} F] , \end{aligned} \quad (\text{B9})$$

and its derivative,

$$\begin{aligned} \frac{\partial}{\partial \Delta} \text{Im} \psi(z) &= \text{Im} \frac{\partial}{\partial \Delta} \psi(z) = \text{Im} \left( \frac{\partial z}{\partial \Delta} \frac{d\psi(z)}{dz} \right) \\ &= \text{Im} \left( i \frac{d\psi(z)}{dz} \right) = \text{Re} \left( \frac{d\psi(z)}{dz} \right) . \end{aligned} \quad (\text{B10})$$

Using Eq. (B6) and Eq. (103), we can write

$$\begin{aligned} \frac{d\psi(z)}{dz} &= \frac{d}{dz} \{ (1 - z^2) [2z - 2(z^2 - 1)^{1/2}] \} \\ &= 2 - 3z [2z - 2(z^2 - 1)^{1/2}] = 2 - 3z F(\eta + i0) , \end{aligned} \quad (\text{B11})$$

so the real part of Eq. (B11) becomes

$$\text{Re} \left( \frac{d\psi(z)}{dz} \right) = \frac{\pi \mathfrak{X} (2\Delta)}{\Delta} - \frac{3\Delta}{\pi \mathfrak{X}} (\eta - \Delta) \text{Re} F - 3\Delta^2 . \quad (\text{B12})$$

Substituting Eqs. (B9), (B10), and (B12) into (B8) yields the equation

$$\begin{aligned} \mathcal{L}(\eta) &= \frac{\pi^2}{4} \frac{\mathfrak{X}}{\Delta} \left( 1 + \frac{2\Delta}{\pi \mathfrak{X}} - 2\Delta^2 - (\eta - \Lambda)^2 \right. \\ &\quad \left. - \frac{\Delta}{\pi \mathfrak{X}} (\eta - \Lambda) \text{Re} F \right) . \end{aligned} \quad (\text{B13})$$

Then Eq. (116) can be used to connect  $\Sigma$  and  $F$ :

$$\Sigma(\eta^*) = \eta - 1/F(\eta^*) - \frac{1}{4} F(\eta^*) , \quad (\text{B14})$$

or, taking the imaginary part of both sides of Eq. (B14), we obtain

$$\Delta = \pi \mathfrak{X} (1/|F|^2 - \frac{1}{4}) . \quad (\text{B15})$$

However, we know that

$$|F|^2 = (\text{Re} F)^2 + \pi^2 \mathfrak{X}^2 . \quad (\text{B16})$$

Solving Eqs. (B15) and (B16) for  $\text{Re} F$ , we get

$$(\text{Re} F)^2 = (\Delta/\pi \mathfrak{X} + \frac{1}{4})^{-1} - \pi^2 \mathfrak{X}^2 . \quad (\text{B17})$$

The real part of (B14) yields

$$\eta - \Lambda = \left( \frac{1}{|F|^2} + \frac{1}{4} \right) \text{Re} F = \left( \frac{\Delta}{\pi \mathfrak{X}} + \frac{1}{2} \right) \text{Re} F . \quad (\text{B18})$$

Substituting  $\eta - \Lambda$  from Eq. (B18) and  $(\text{Re} F)^2$  from (B17) into Eq. (B13), and collecting terms, yields

$$\mathcal{L}(\eta) = \frac{\pi^4 \mathfrak{X}^3}{16\Delta} \left( 1 + \frac{6\Delta}{\pi \mathfrak{X}} \right) . \quad (\text{B19})$$

#### APPENDIX C: VIRTUAL-CRYSTAL LIMIT

In the notation of Sec. VD, the scattering strength is defined by  $\mathcal{E}_A = \frac{1}{2} \delta$ ,  $\mathcal{E}_B = -\frac{1}{2} \delta$ . In the weak-scattering limit  $\delta \ll 1$  and  $\alpha_A$  and  $\alpha_B \ll 1$ , so a perturbation expansion in powers of these parameters is useful. The CPA self-energy  $\Sigma$  can be expressed as

$$\Sigma = \langle\langle \mathcal{E}_n + \theta_n \rangle\rangle + \langle\langle (\mathcal{E}_n + \theta_n) F \tau_n \rangle\rangle , \quad (\text{C1})$$

where  $\tau_n$  is the site-diagonal matrix element of  $T_n$  [see Eq. (66)], i. e. ,

$$\begin{aligned} \tau_n &= \frac{\mathcal{E}_n + \theta_n - \Sigma}{1 - (\mathcal{E}_n + \theta_n - \Sigma) F} \\ &= \mathcal{E}_n + \theta_n - \Sigma + (\mathcal{E}_n + \theta_n - \Sigma) F (\mathcal{E}_n + \theta_n - \Sigma) + \dots . \end{aligned} \quad (\text{C2})$$

Let us evaluate the first three  $\Sigma^{(i)}$ , defined as  $\Sigma$  correct to powers of  $\delta^i$  and  $\alpha^{i/2}$  in CPA. The first three moments of  $\langle\langle (\mathcal{E}_n + \theta_n)^i \rangle\rangle$  are

$$\begin{aligned} \langle\langle \mathcal{E}_n + \theta_n \rangle\rangle &= (x - y) \delta / 2 \equiv \bar{\epsilon} , \\ \langle\langle (\mathcal{E}_n + \theta_n)^2 \rangle\rangle &= \frac{1}{4} \delta^2 + x \alpha_A + y \alpha_B , \\ \langle\langle (\mathcal{E}_n + \theta_n)^3 \rangle\rangle &= (x - y) \delta / 8 + \frac{3}{2} x \delta \alpha_A - \frac{3}{2} y \delta \alpha_B . \end{aligned} \quad (\text{C3})$$

The first three self-energies are

$$\begin{aligned} \Sigma^{(0)} &= 0 , \\ \Sigma^{(1)} &= \langle\langle \mathcal{E}_n + \theta_n \rangle\rangle = \bar{\epsilon} , \\ \Sigma^{(2)} &= \langle\langle \mathcal{E}_n + \theta_n \rangle\rangle + \langle\langle (\mathcal{E}_n + \theta_n)^2 \rangle\rangle F - \langle\langle \mathcal{E}_n + \theta_n \rangle\rangle \Sigma^{(1)} F \end{aligned}$$

$$\begin{aligned}
&= \bar{\epsilon} + (\frac{1}{4}\delta^2 + x\alpha_A + y\alpha_B)F - \bar{\epsilon}^2 F \\
&= \bar{\epsilon} + (xy\delta^2 + x\alpha_A + y\alpha_B)F .
\end{aligned} \tag{C4}$$

In Eq. (C4),  $F$  must be correct to order of  $\delta^1$  and  $\alpha^{1/2}$ . The density of states per atom  $\mathfrak{N}(E)$  is then approximated by

$$\begin{aligned}
\mathfrak{N}(E) &= -(1/\pi)\text{Im}F(E+i0) \\
&= -(1/\pi)\text{Im}F_0(E+i0 - \Sigma(E+i0)) \\
&\simeq -(1/\pi)\text{Im}F_0(E - \bar{\epsilon}) = \mathfrak{N}_0(E - \bar{\epsilon}) ,
\end{aligned} \tag{C5}$$

which is just the ‘‘rigid-band-model’’ result. To the lowest order, according to Eq. (112), the conductivity is

$$\sigma \simeq \frac{\pi^2 e^2 \hbar v_m^2}{12\Omega_c} \frac{\mathfrak{N}_0^3(\epsilon_F - \bar{\epsilon})}{\Delta(\epsilon_F)} , \tag{C6}$$

and the resistivity is

$$\begin{aligned}
\rho &= \frac{12\Omega_c}{\pi^2 e^2 \hbar v_m^2} \frac{\Delta(\epsilon_F)}{\mathfrak{N}_0^3(\epsilon_F - \bar{\epsilon})} \\
&\simeq \frac{12\Omega_c}{\pi e^2 \hbar v_m^2} \frac{xy\delta^2 + x\alpha_A + y\alpha_B}{\mathfrak{N}_0^2(\epsilon_F - \bar{\epsilon})} .
\end{aligned} \tag{C7}$$

Equation (C7) exhibits Matthiessen’s rule,

$$\rho = \rho_I + \rho_p , \tag{C8}$$

with

$$\rho_I = \frac{12\Omega_c}{\pi e^2 \hbar v_m^2} \frac{xy\delta^2}{\mathfrak{N}_0^2(\epsilon_F - \bar{\epsilon})} , \tag{C9}$$

and

$$\rho_p = \frac{12\Omega_c}{\pi e^2 \hbar v_m^2} \frac{x\alpha_A + y\alpha_B}{\mathfrak{N}_0^2(\epsilon_F - \bar{\epsilon})} . \tag{C10}$$

The ‘‘impurity’’ contribution  $\rho_I$  then obeys the Nordheim rule,<sup>73</sup> because  $\rho_I \propto xy\delta^2$ . The ‘‘electron-phonon’’ contribution to resistivity,  $\rho_p$ , has a slope as a function of  $T$  which lies between those of the pure crystals.

#### APPENDIX D: A PERTURBATION SOLUTION FOR $F$ AND $\Sigma$

The self-consistent equation for  $F$  [Eq. (124)] is

$$F = xI_A + yI_B \tag{D1}$$

where

$$\begin{aligned}
I_{A,B} &\equiv \int d\eta \frac{1}{(2\pi\alpha_{A,B})^{1/2}} e^{-\eta^2/2\alpha_{A,B}} \\
&\quad \times (z - \epsilon_{A,B} - \eta - \frac{1}{4}F)^{-1} .
\end{aligned} \tag{D2}$$

Let  $\alpha_A = \gamma\alpha$  and  $\alpha_B = \alpha$ . If  $\alpha \ll 1$ , and  $F$  is very close to the static-alloy value  $F^{(0)}$ , we can use a perturbation method to solve for  $F$ :

$$\begin{aligned}
F &= F^{(0)} + F^{(1)}\alpha + \dots , \\
I_{A,B} &= I_{A,B}^{(0)} + I_{A,B}^{(1)}\alpha + \dots ,
\end{aligned} \tag{D3}$$

where

$$I_{A,B}^{(0)} = \lim_{\alpha \rightarrow 0} I_{A,B}(\alpha) = \frac{1}{z - \mathcal{E}_{A,B} - \frac{1}{4}F} , \tag{D4}$$

and

$$I_{A,B}^{(1)} = \left( \frac{\partial I_{A,B}}{\partial \alpha} + \frac{\partial I_{A,B}}{\partial F} \frac{\partial F}{\partial \alpha} \right) \Big|_{\alpha=0} . \tag{D5}$$

The zeroth-order equation

$$F^{(0)} = \frac{x}{z - \mathcal{E}_A - \frac{1}{4}F^{(0)}} + \frac{y}{z - \mathcal{E}_B - \frac{1}{4}F^{(0)}} \tag{D6}$$

is just the self-consistent equation for the static-alloy  $F^{(0)}$ . The first-order equation is

$$\begin{aligned}
F^{(1)} &= xI_A^{(1)} + yI_B^{(1)} \\
&= \frac{x\gamma}{(z - \mathcal{E}_A - \frac{1}{4}F^{(0)})^3} + \frac{F^{(1)}}{4} \frac{x}{(z - \mathcal{E}_A - \frac{1}{4}F^{(0)})^2} \\
&\quad + \frac{y}{(z - \mathcal{E}_B - \frac{1}{4}F^{(0)})^3} + \frac{F^{(1)}}{4} \frac{y}{(z - \mathcal{E}_B - \frac{1}{4}F^{(0)})^2} .
\end{aligned} \tag{D7}$$

The solution for  $F^{(1)}$  is then

$$F^{(1)} = \frac{x\gamma h_B^3 + y h_A^3}{h_A^3 h_B^3 - \frac{1}{4}x h_A h_B^3 - \frac{1}{4}y h_B h_A^3} , \tag{D8}$$

where

$$h_{A,B} \equiv z - \mathcal{E}_{A,B} - \frac{1}{4}F^{(0)} . \tag{D9}$$

Using the identity, Eq. (116), we can solve for  $\Sigma$  by letting

$$\Sigma = \Sigma^{(0)} + \Sigma_\alpha^{(1)}\alpha + \dots . \tag{D10}$$

Then we find

$$\Sigma_\alpha^{(1)} = \left( \frac{1}{(F^{(0)})^2} - \frac{1}{4} \right) F^{(1)} . \tag{D11}$$

#### APPENDIX E: CPA DENSITY OF STATES AND CONDUCTIVITY IN TERMS OF SELF-ENERGY IN FREE-ELECTRON MODEL

In the free-electron model, the unperturbed density of states per atom,  $\mathfrak{N}_0(E)$ , is simply

$$\mathfrak{N}_0(E) = \left( \frac{1}{2} \right)^{1/2} \frac{\Omega}{N\pi^2} \frac{m^{3/2}}{\hbar} E^{1/2} \equiv A E^{1/2} . \tag{E1}$$

The CPA density of states per atom,  $N(E)$ , in terms of the self-energy  $\Sigma(E)$ , is

$$\begin{aligned}
\mathfrak{N}(E) &= \frac{1}{\pi N} \sum_{\mathbf{k}} \frac{\Delta(E)}{[E - \Lambda(E) - \epsilon(\mathbf{k})]^2 + \Delta^2(E)} \\
&= \frac{1}{\pi} \int_0^\infty d\epsilon \frac{\mathfrak{N}_0(\epsilon)\Delta(E)}{[E - \Lambda(E) - \epsilon]^2 + \Delta^2(E)} ,
\end{aligned} \tag{E2}$$

where  $\Sigma(E \pm i0) = \Lambda(E) \mp i\Delta(E)$  as usual. Using Eq. (E1), we can rewrite  $\mathfrak{N}(E)$  as

$$\mathfrak{N}(E) = A[\Delta(E)/\pi] Y(E) , \tag{E3}$$



where  $Y(E)$  is the integral

$$Y(E) = \int_0^\infty \frac{\epsilon^{1/2} d\epsilon}{[E - \Lambda(E) - \epsilon]^2 + \Delta^2(E)}. \quad (\text{E4})$$

This integral is easily carried out using a contour sketched in Fig. 10. Let us define  $\beta = E - \Lambda(E)$ ,  $\rho = (\beta^2 + \Delta^2)^{1/2}$ , and  $\theta = \tan^{-1}(\Delta/\beta)$ . Then it terms of residues,

$$Y(E) = \pi i \left( \frac{(\beta + i\Delta)^{1/2}}{2i\Delta} + \frac{(\beta - i\Delta)^{1/2}}{-2i\Delta} \right) \\ = (\pi/\Delta)\rho^{1/2} \cos \frac{1}{2}\theta = (\pi/\Delta) \left[ \frac{1}{2}(\rho + \beta) \right]^{1/2}. \quad (\text{E5})$$

Thus  $\mathfrak{X}(E)$  becomes

$$\mathfrak{X}(E) = (A/\sqrt{2}) \{ [(E - \Lambda(E))^2 + \Delta^2]^{1/2} + E - \Lambda(E) \}^{1/2}. \quad (\text{E6})$$

The CPA conductivity  $\sigma$  according to Eq. (99) is

$$\sigma = \frac{2e^2\hbar}{\pi\Omega_c} \int d\eta \left( -\frac{df}{d\eta} \right) \int d\xi \left[ \left( \frac{\Delta(\eta)}{[\eta - \xi - \Lambda(\eta)]^2 + \Delta^2(\eta)} \right)^2 \frac{1}{3N} \sum_{\mathbf{k}} v^2(\mathbf{k}) \delta(\xi - \epsilon(\mathbf{k})) \right]. \quad (\text{E7})$$

Since the velocity dispersion  $v^2(m)$  is simply

$$v^2(\mathbf{k}) = \frac{\hbar^2 k^2}{m^2} = \frac{2\epsilon(\mathbf{k})}{m} = \frac{2}{mA^2} N_0^2(\epsilon(\mathbf{k})), \quad (\text{E8})$$

the conductivity is

$$\sigma = \frac{2e^2\hbar}{\pi\Omega_c} \frac{2}{3m} \int d\eta \left( -\frac{df}{d\eta} \right) \int d\xi \\ \times \frac{N_0(\xi)\xi\Delta^2(\eta)}{[\eta - \Lambda(\eta) - \xi]^2 + \Delta^2(\eta)^2}. \quad (\text{E9})$$

Using Eq. (E1) for  $N_0(\xi)$ , we get

$$\sigma = \frac{2e^2\hbar}{\pi\Omega_c} \frac{2A}{3m} \int d\eta \left( -\frac{df}{d\eta} \right) I(\eta)\Delta^2(\eta) \\ \approx \frac{4e^2\hbar A}{3\pi\Omega_c m} \Delta^2(\epsilon_F) I(\epsilon_F), \quad (\text{E10})$$

where

$$I(\epsilon_F) \equiv \int_0^\infty d\epsilon \frac{\epsilon^{3/2}}{[\epsilon_F - \Lambda(\epsilon_F) - \epsilon]^2 + \Delta^2(\epsilon_F)^2}. \quad (\text{E11})$$

Using the same contour as in Fig. 10, and the notation of Eq. (E5), we can write  $I(\epsilon_F)$  in terms of the residues of the double poles,

$$I = \pi i [\text{Res}(\beta + i\Delta) + \text{Res}(\beta - i\Delta)], \quad (\text{E12})$$

where

$$\text{Res}(\beta + i\Delta) = \frac{3}{2} \frac{(\beta + i\Delta)^{1/2}}{(2i\Delta)^2} - 2 \frac{(\beta + i\Delta)^{3/2}}{(2i\Delta)^3}. \quad (\text{E13})$$

Treating the  $\text{Res}(\beta - i\Delta)$  similarly, the integral  $I$

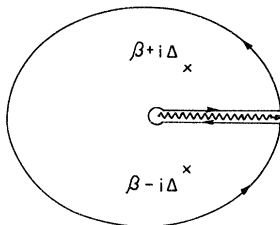


FIG. 10. Contour for the integrations in Eqs. (E3) and (E11).

becomes

$$I = \frac{3\pi}{4\Delta^2} \left[ \frac{1}{2}(\rho - \beta) \right]^{1/2} \\ + \frac{\pi}{2\Delta^3} \{ \beta \left[ \frac{1}{2}(\rho + \beta) \right]^{1/2} - \Delta \left[ \frac{1}{2}(\rho - \beta) \right]^{1/2} \} \\ = \frac{\pi}{4\Delta^2} \left[ \frac{1}{2}(\rho - \beta) \right]^{1/2} + \frac{\pi}{2\Delta^3} \beta \left[ \frac{1}{2}(\rho + \beta) \right]^{1/2}. \quad (\text{E14})$$

Thus we find from Eqs. (E10) and (E14),

$$\sigma = \frac{2e^2\hbar A}{3\Omega_c m} \frac{1}{\Delta} \{ \beta \left[ \frac{1}{2}(\beta + \rho) \right]^{1/2} + \frac{1}{2} \Delta \left[ \frac{1}{2}(\rho - \beta) \right]^{1/2} \}. \quad (\text{E15})$$

Using the result of Eqs. (E4) and (E5), we can see that  $\mathfrak{X} = A \left[ \frac{1}{2}(\beta + \rho) \right]^{1/2}$ . Then  $\sigma$  becomes

$$\sigma = \frac{2e^2\hbar A}{3\Omega_c m} \frac{1}{\Delta} \left[ \frac{1}{2}(\beta + \rho) \right]^{1/2} \left( \beta + \frac{\Delta}{2} \frac{\rho - \beta}{(\rho^2 - \beta^2)^{1/2}} \right) \\ = \frac{2e^2\hbar A}{3\Omega_c m} \frac{1}{\Delta} \left[ \frac{1}{2}(\beta + \rho) \right]^{1/2} \left[ \frac{1}{2}(\rho + \beta) \right] \\ = \frac{2e^2\hbar A}{3\Omega_c m} \frac{1}{\Delta} \left[ \frac{1}{2}(\beta + \rho) \right]^{3/2} \\ = \frac{2e^2\hbar}{3\Omega_c mA^2} \frac{\mathfrak{X}^3(\epsilon_F)}{\Delta(\epsilon_F)}. \quad (\text{E16})$$

Note that this result is identical with Eq. (112) providing that  $\Delta/\mathfrak{X}$  is taken to be zero, which it is when an infinite half-bandwidth is used as the energy unit. Thus, strong scattering here is identical with weak scattering in the finite band. Naturally, if the scatterers are attractive, they must not contain bound states, or the theory based on a one-band model is inappropriate.

#### APPENDIX F: FERMİ VELOCITY

The averaged square of the velocity of electrons at the Fermi energy  $\epsilon_F$  in an alloy is

$$\langle\langle v^2(\epsilon_F) \rangle\rangle = \text{Tr} \langle\langle (p/m)^2 \delta(\epsilon_F - H) \rangle\rangle [\text{Tr} \langle\langle \delta(\epsilon_F - H) \rangle\rangle]^{-1}. \quad (\text{F1})$$

In a single-band model, this can be written as

$$\langle\langle v^2(\epsilon_F) \rangle\rangle = \frac{1}{\pi N \mathfrak{N}(\epsilon_F)} \sum_{\vec{k}} v^2(\vec{k}) |\text{Im} g(\vec{k}, \epsilon_F \pm i0)|, \quad (\text{F2})$$

where

$$v^2(\vec{k}) = \sum_{\alpha} [v^{\alpha}(\vec{k})]^2 \quad (\text{F3})$$

and  $g(\vec{k}, z)$  is defined in Eq. (74).

In CPA and our model, the self-energy is independent of  $\vec{k}$ . In terms of the self-energy,  $\langle\langle v^2(\epsilon_F) \rangle\rangle$  becomes

$$\begin{aligned} \langle\langle v^2(\epsilon_F) \rangle\rangle &= \frac{1}{\pi N \mathfrak{N}} \sum_{\vec{k}} \frac{v^2(\vec{k}) \Delta(\epsilon_F)}{[\epsilon_F - \epsilon(\vec{k}) - \Lambda(\epsilon_F)]^2 + \Delta^2(\epsilon_F)} \\ &= \frac{1}{\pi \mathfrak{N}} \int d\xi \left( \frac{\Delta}{(\epsilon_F - \xi - \Lambda)^2 + \Delta^2} \right. \\ &\quad \left. \times \frac{1}{N} \sum_{\vec{k}} v^2(\vec{k}) \delta(\xi - \epsilon(\vec{k})) \right) \\ &= \frac{1}{\pi \mathfrak{N}} \int d\xi \frac{\Delta v^2(\xi) \mathfrak{N}_0(\xi)}{(\epsilon_F - \xi - \Lambda)^2 + \Delta^2} \\ &= \frac{2 \Delta v_m^2}{\pi^2 \mathfrak{N}} \int d\xi \frac{(1 - \xi^2)^{3/2}}{(\epsilon_F - \xi - \Lambda)^2 + \Delta^2}. \quad (\text{F4}) \end{aligned}$$

In Eq. (F4), we have used the definition of the velocity dispersion  $v^2(\xi)$  from Eq. (100), the model velocity  $v^2$  from Eq. (107) and the model density of states from Eq. (102). Using the definitions for  $z$ ,  $\psi$  [Eq. (B6)], and  $\Phi$  [Eq. (B7)] in Appendix B, we can express  $\langle\langle v^2(\eta) \rangle\rangle$  as

$$\begin{aligned} \langle\langle v^2(\eta) \rangle\rangle &= \frac{-2v_m^2}{\pi^2 \mathfrak{N}} \text{Im} \left( \int_{-1}^1 d\xi \frac{(1 - \xi^2)^{3/2}}{z - \xi} \right) \\ &= \frac{-2v_m^2}{\pi^2 \mathfrak{N}} \text{Im} \Phi(z) = -\frac{2v_m^2}{\pi^2 \mathfrak{N}} \frac{\pi}{2} [z - \psi(z)] \\ &= -\frac{v_m^2}{\pi \mathfrak{N}} \left[ \Delta - \pi \mathfrak{N} \left( 1(\eta - \Lambda)^2 + \Delta^2 + \frac{2\Delta}{\pi \mathfrak{N}} (\eta - \Lambda) \text{Re} F \right) \right]. \quad (\text{F5}) \end{aligned}$$

In Eq. (F5), we have used the explicit expression for  $\text{Im} \psi$  from Eq. (B9). Again, using the results in Appendix B, i. e., Eq. (B18) for  $\eta - \Lambda$  and Eq. (B17) for  $\text{Re} F$ , we find

$$\langle\langle v^2(\epsilon_F) \rangle\rangle = v_m^2 \left[ \frac{\pi^2 \mathfrak{N}(\epsilon_F)}{4} + 3 \frac{\Delta(\epsilon_F)}{\pi \mathfrak{N}(\epsilon_F)} \left( 1 + \frac{4\Delta(\epsilon_F)}{\pi \mathfrak{N}(\epsilon_F)} \right)^{-1} \right]. \quad (\text{F6})$$

#### APPENDIX G: SOME ANALYTIC CPA RESULTS FOR 50-50 ALLOYS, WITH $\alpha_A = \alpha_B$ , AT THE CENTER OF THE BAND $E = 0$

##### 1. $F^{(0)}$ , $\Sigma^{(0)}$ , and $\mathfrak{N}^{(0)}$

For  $x = 0.5$  and  $E = 0$ ,  $F^{(0)}$  satisfies [see Eq. (117)]

$$\frac{1}{16} (F^{(0)})^3 - \frac{1}{4} (\delta^2 - 1) F^{(0)} = 0. \quad (\text{G1})$$

There is no complex solution for  $\delta > 1$ . For  $\delta < 1$ , we choose the solution corresponding to  $F^{(0)}(i0)$ ,

$$F^{(0)}(i0) = -2i(1 - \delta^2)^{1/2}, \quad (\text{G2})$$

so that from Eq. (61)

$$\mathfrak{N}^{(0)}(0) = (2/\pi)(1 - \delta^2)^{1/2}, \quad (\text{G3})$$

and from Eq. (116),

$$\Sigma^{(0)}(i0) = -\frac{1}{F^{(0)}} - \frac{1}{4} F^{(0)} = \frac{-\delta^2 i}{2(1 - \delta^2)^{1/2}}. \quad (\text{G4})$$

##### 2. Changes in $\Delta(0)$ and $\mathfrak{N}(0)$ due to Small Thermal Fluctuations

Let us evaluate  $F^{(1)}$  [Eq. (D8)] in the simple case:

$$F^{(1)}(i0) = \frac{1}{2} \frac{(h_A + h_B)(h_A^2 + h_B^2 - h_A h_B)}{h_A h_B (h_A^2 h_B^2 - \frac{1}{8} h_A^2 - \frac{1}{8} h_B^2)}. \quad (\text{G5})$$

Here,  $h_{A,B}$  take the values [see Eqs. (D9) and (G2)]

$$h_A = -\frac{1}{2} \delta + \frac{1}{2} i(1 - \delta^2)^{1/2}, \quad (\text{G6})$$

and

$$h_B = \frac{1}{2} \delta + \frac{1}{2} i(1 - \delta^2)^{1/2},$$

so that

$$F^{(1)}(i0) = -16i(\delta^2 - \frac{1}{4})/(1 - \delta^2)^{1/2}. \quad (\text{G7})$$

Then the change in density of states is

$$\mathfrak{N}(0) - \mathfrak{N}^{(0)}(0) = \frac{-1}{\pi} \text{Im} F^{(1)}(i0) \alpha = \frac{16}{\pi} \frac{(\delta^2 - \frac{1}{4}) \alpha}{(1 - \delta^2)^{1/2}}, \quad (\text{G8})$$

and the change in  $\Delta$  can be obtained by using Eqs. (D11), (G2), and (G7)

$$\Delta(0) - \Delta^{(0)}(0) = -\text{Im} \Sigma_{\alpha}^{(1)}(i0) \alpha = \frac{-4(2 - \delta^2)(\delta^2 - \frac{1}{4}) \alpha}{(1 - \delta^2)^{3/2}}. \quad (\text{G9})$$

Thus, the changes in  $\Delta$  and  $\mathfrak{N}$  go in opposite directions. The change in  $\Delta$  is negative for  $1 > \delta > \frac{1}{2}$ , and positive for  $\delta < \frac{1}{2}$ .

##### 3. Fermi Velocity for Static Alloy

Using the results for  $\mathfrak{N}^{(0)}(0)$  [Eq. (G2)] and  $\Delta^{(0)}(0)$  [see Eq. (G4)], we have a simple expression for the Fermi velocity  $\langle\langle v^2(0) \rangle\rangle$  appearing in Appendix F:

$$\begin{aligned} \langle\langle v^2(0) \rangle\rangle &= v_m^2 \left[ (1 - \delta^2) + 3 \frac{\delta^2}{4(1 - \delta^2)} \left( 1 + \frac{\delta^2}{1 - \delta^2} \right)^{-1} \right] \\ &= v_m^2 (1 - \frac{1}{4} \delta^2). \quad (\text{G10}) \end{aligned}$$

- \*Work supported by NASA under Grant Nos. NGR-47-006-045 and NSF-GU-3842.
- †Part of this work was done while in residence at the Aspen Center for Physics.
- <sup>1</sup>A collection of experimental data for thermal properties of alloys can be found in *Thermophysical Properties of High Temperature Solid Materials*, edited by Y. S. Touloukian (Purdue U. P., LaFayette, Ind., 1967), Vols. II and III.
- <sup>2</sup>For example, G. T. Meaden, *Electrical Resistance of Metals* (Plenum, New York, 1965).
- <sup>3</sup>M. M. Lemcoe (private communication).
- <sup>4</sup>B. Velický, S. Kirkpatrick, and H. Ehrenreich, Phys. Rev. 175, 747 (1968).
- <sup>5</sup>S. Kirkpatrick, B. Velický, and H. Ehrenreich, Phys. Rev. B 1, 3250 (1970).
- <sup>6</sup>G. W. Stocks, R. W. Williams, and J. S. Faulkner, Phys. Rev. Letters 26, 253 (1971).
- <sup>7</sup>K. Levin and H. Ehrenreich, Phys. Rev. B 3, 4172 (1971).
- <sup>8</sup>Paul Soven, Phys. Rev. 156, 809 (1967).
- <sup>9</sup>B. Velický, Phys. Rev. 184, 614 (1969).
- <sup>10</sup>R. E. Peierls, *Quantum Theory of Solids* (Clarendon Press, Oxford, England, 1955), pp. 139-142.
- <sup>11</sup>L. Van Hove, Physica 21, 517 (1955); 23, 441 (1957).
- <sup>12</sup>W. Kohn and J. M. Luttinger, Phys. Rev. 108, 590 (1957).
- <sup>13</sup>J. M. Luttinger and W. Kohn, Phys. Rev. 109, 1892 (1958).
- <sup>14</sup>R. Kubo, J. Phys. Soc. Japan 12, 570 (1957).
- <sup>15</sup>R. Kubo, *Lectures in Theoretical Physics* (Interscience, New York, 1958), Vol. 1, p. 121.
- <sup>16</sup>E. J. Moore, Phys. Rev. 160, 607 (1967).
- <sup>17</sup>E. Verboven, Physica 36, 1091 (1960).
- <sup>18</sup>D. A. Greenwood, Proc. Phys. Soc. (London) 71, 585 (1958).
- <sup>19</sup>S. F. Edwards, Advan. Phys. 16, 359 (1967).
- <sup>20</sup>See, for example, W. Heitler, *The Quantum Theory of Radiation* (Oxford U. P., Oxford, England, 1954), p. 69.
- <sup>21</sup>G. V. Chester and A. Thellung, Proc. Phys. Soc. (London) 73, 745 (1959).
- <sup>22</sup>N. F. Mott, Advan. Phys. 16, 49 (1967).
- <sup>23</sup>M. H. Cohen, J. Non-Cryst. Solids 41, 391 (1970).
- <sup>24</sup>M. H. Cohen, Phys. Today 24 (No. 5), 26 (1971).
- <sup>25</sup>S. F. Edwards, Phil. Mag. 6, 617 (1961).
- <sup>26</sup>T. E. Faber and J. M. Ziman, Phil. Mag. 11, 153 (1965).
- <sup>27</sup>A. B. Bhatia and D. E. Thornton, Phys. Rev. B 2, 3004 (1970).
- <sup>28</sup>N. F. Mott and H. Jones, *Theory of Properties of Metals and Alloys* (Dover, New York, 1958).
- <sup>29</sup>S. F. Edwards, Phil. Mag. 3, 1020 (1958).
- <sup>30</sup>J. S. Langer, Phys. Rev. 120, 714 (1960); 124, 1003 (1961); 127, 5 (1962).
- <sup>31</sup>For example, A. A. Abrikosov, L. P. Gorkov, and I. Ye Dzyaloshinskii, *Quantum Field Theoretical Methods in Statistical Physics*, 2nd ed. (Pergamon, New York, 1965).
- <sup>32</sup>J. L. Beeby, Phys. Rev. 135, A130 (1964).
- <sup>33</sup>L. E. Ballentine, Can. J. Phys. 44, 2533 (1966).
- <sup>34</sup>D. W. Taylor, Phys. Rev. 156, 1017 (1967).
- <sup>35</sup>Y. Onodera and Y. Toyozawa, J. Phys. Soc. Japan 24, 341 (1968).
- <sup>36</sup>F. Yonezawa, Progr. Theoret. Phys. (Kyoto) 40, 734 (1968).
- <sup>37</sup>J. M. Ziman, J. Phys. C 2, 1230 (1969).
- <sup>38</sup>T. Matsubara and Y. Toyozawa, Progr. Theoret. Phys. (Kyoto) 26, 739 (1961).
- <sup>39</sup>P. L. Leath, Phys. Rev. B 2, 3078 (1970).
- <sup>40</sup>N. F. Berk, Phys. Rev. B 1, 1336 (1970).
- <sup>41</sup>S. F. Edwards and J. M. Loveluck, J. Phys. C 3, S261 (1970).
- <sup>42</sup>K. F. Freed and M. H. Cohen, Phys. Rev. B 3, 3400 (1971).
- <sup>43</sup>W. Kohn, in *Proceedings of the Third IMR Symposium on Electronic Density of States*, Natl. Bur. Std. Spec. Publ. No. 323 (U. S. GPO, Washington, D. C., 1970).
- <sup>44</sup>I. M. Lifshitz, Usp. Fiz. Nauk 83, 617 (1964) [Sov. Phys. Usp. 7, 549 (1965)].
- <sup>45</sup>P. W. Anderson and W. L. McMillan, in *Theory of Magnetism in Transition Metals, Proceedings of the International School of Physics "Enrico Fermi", Course 37*, edited by H. Suhl (Academic, New York, 1967), p. 60.
- <sup>46</sup>Paul Soven, Phys. Rev. B 2, 4715 (1970).
- <sup>47</sup>S. Kirkpatrick, B. Velický, N. D. Lang, and H. Ehrenreich, J. Appl. Phys. 40, 1283 (1969).
- <sup>48</sup>B. Velický and K. Levin, Phys. Rev. B 2, 4 (1970); 2, 938 (1970).
- <sup>49</sup>The formalism of CPA in this section follows closely to that given in Refs. 4 and 9.
- <sup>50</sup>Reference 9, Eq. (118). Note the difference in the definition of  $\Lambda$ .
- <sup>51</sup>L. J. Sham and J. M. Ziman, in *Solid State Physics*, edited by F. Seitz and D. Turnbull (Academic, New York, 1963), Vol. 15. There is a demonstration of some cancellation between the multiple-phonon processes and the Debye-Waller factor. This allows us to use the one-phonon interaction Hamiltonian and ignore multiple-phonon processes.
- <sup>52</sup>A. Messiah, *Quantum Mechanics* (Wiley, New York, 1966), Vol. 1, p. 448.
- <sup>53</sup>J. Hubbard, Proc. Roy. Soc. (London) A281, 401 (1964).
- <sup>54</sup>*Handbook of Mathematical Functions*, edited by M. Abramowitz and I. A. Stegun (Natl. Bur. Std., U. S. GPO, Washington, D. C., 1964), p. 297.
- <sup>55</sup>Reference 54, Eq. (7.1.8).
- <sup>56</sup>V. I. Krylov, *Approximate Calculation of Integrals* (MacMillan, New York, 1962), pp. 129-130 and 343-346.
- <sup>57</sup>Paul Soven, Phys. Rev. 178, 1136 (1969).
- <sup>58</sup>J. M. Ziman, *The Physics of Metals* (Cambridge U. P., Cambridge, England, 1969), Vol. 1, Chap. 5; Advan. Phys. 16, 551 (1967).
- <sup>59</sup>L. F. Mattheis, Phys. Rev. 134, A970 (1964).
- <sup>60</sup>V. Heine, Phys. Rev. 153, 673 (1967).
- <sup>61</sup>R. E. Watson, H. Ehrenreich, and L. Hodges, Phys. Rev. Letters 24, 829 (1970).
- <sup>62</sup>J. S. Kouvel and J. B. Comly, Phys. Rev. Letters 24, 598 (1970).
- <sup>63</sup>See the density of states curve in L. Hodges, H. Ehrenreich, and N. D. Lang, Phys. Rev. 152, 505 (1966).
- <sup>64</sup>Paul Soven (private communication).
- <sup>65</sup>T. J. Hicks, B. Rainford, J. S. Kouvel, G. G. Low, and J. B. Comly, Phys. Rev. Letters 22, 531 (1969).
- <sup>66</sup>See the review paper by J. Kondo, in *Solid State Physics*, edited by F. Seitz and D. Turnbull (Academic, New York, 1969), Vol. 23, p. 183.
- <sup>67</sup>G. Weisz (unpublished).
- <sup>68</sup>K. S. Chang (private communication).

<sup>69</sup>G. D. Whitfield, Phys. Rev. 121, 720 (1961); or Ref. 50.  
<sup>70</sup>J. M. Ziman, *Principles of the Theory of Solids* (Cambridge U.P., Cambridge, England, 1965), p. 188, Eq. (7.52).

<sup>71</sup>See Ref. 70, Eq. (7.54) and Ref. 51, Eq. (2.10).  
<sup>72</sup>V. Heine, in *The Physics of Metals*, edited by J. Ziman (Cambridge U.P., Cambridge, England, 1969), Vol. 1, Chap. 1, Eq. (1.55).  
<sup>73</sup>L. Nordheim, Ann. Phys. (N.Y.) 9, 607 (1931).

PHYSICAL REVIEW B

VOLUME 5, NUMBER 8

15 APRIL 1972

## Transport Properties and the Electronic Structure of $\text{LaSn}_{3-x}\text{In}_x$

Warren D. Grobman

*IBM Thomas J. Watson Research Center, Yorktown Heights, New York 10598*

(Received 29 July 1971)

Measurements of resistivity, magnetoresistance, and thermopower were made on a series of compounds of the type  $\text{LaSn}_{3-x}\text{In}_x$  for temperatures from 1.5 to over 300 K. In addition, Hall effect in  $\text{LaIn}_3$  was measured from 10 to 270 K. These experiments are interpreted in the light of previous data on these compounds with the object of obtaining a better understanding of their electronic structure. The main conclusions are that these compounds are transition metals which possess neither local moments nor magnetic phase transitions. They contain small pockets of electrons near the Fermi surface for  $x=0$  which disappear as  $x$  approaches unity. This result is consistent with measurements of magnetic susceptibilities and superconducting properties. Finally, arguments are presented based on thermopower measurements which indicate that Ce in  $\text{LaIn}_3$  is a Kondo system.

### I. INTRODUCTION

Intermetallic compounds of the form  $\text{LaX}_{3-x}\text{Y}_x$  with X or Y representing Sn, In, Pb, or Tl have been studied extensively in recent years.<sup>1-8</sup> These papers have been motivated by the possibility of studying superconductivity and magnetism as a function of electron or rare-earth impurity concentration in these compounds. The  $\text{LaX}_{3-x}\text{Y}_x$  compounds are also easy to work with experimentally as they possess a simple crystal structure (simple-cubic Bravais lattice), are single phase, congruently melting, and can be grown as large single crystals.<sup>1</sup>

As a result of the previous work on these materials, several questions concerning their electronic structure have arisen. The dramatic variation<sup>8</sup> of  $T_c$  with  $x$  near  $x=0$  in  $\text{LaSn}_{3-x}\text{In}_x$ , as well as the unusual results for  $\chi(T)$  in  $\text{LaSn}_3$  has led to speculation that  $\text{LaSn}_3$  possesses local moments or strong exchange enhancement.<sup>5</sup> Here  $T_c$  is the superconducting critical temperature and  $\chi(T)$  is the magnetic susceptibility as a function of absolute temperature  $T$ .

Havinga *et al.*<sup>6</sup> have done an extensive series of experiments on  $T_c$ ,  $\chi(300\text{ K})$ , and  $S(300\text{ K})$  vs electron concentration in these compounds, where  $S$  is the thermopower. The oscillations in these quantities plotted as a function of electron concentration have been ascribed by them to expansion of a simple-metal Fermi surface through a Brillouin-zone boundary as electron concentration is in-

creased. In addition, they interpret  $S_x(300\text{ K})$  vs  $x$  by assuming that umklapp processes dominate the thermopower. (In the present paper a subscript  $x$  denotes a property measured as a function of the concentration  $x$  of In in  $\text{LaSn}_{3-x}\text{In}_x$ .)

The present measurements of transport properties in  $\text{LaSn}_{3-x}\text{In}_x$  vs  $x$  were performed in order to test these ideas and to clarify our understanding of the electronic structure of these compounds. We have measured  $\rho(H)$ ,  $\rho(T)$ , and  $S(T)$  vs  $x$  for  $1.2 \leq T \leq 350\text{ K}$  ( $\rho$  is the resistivity), and in  $\text{LaIn}_3$  have measured the low-field Hall coefficient  $R_H$  for  $10 \leq T \leq 270\text{ K}$ . The behavior of  $\rho(H)$  and  $\rho(T)$  has led to the conclusion that these compounds do not possess local moments nor magnetic phase transitions as a function of  $x$  or  $T$ . Low-temperature measurements of  $\rho(T)$  have led us to reject the suggestion<sup>6</sup> that these materials are simple metals, while  $S_x$  for different temperatures suggests that the behavior of  $S$  vs  $x$  is not explainable on the basis of umklapp processes. Rather, the present measurements, especially  $\rho_x(H)$  for  $0 < x < 1$ , suggest that the unusual behavior of  $\text{LaSn}_{3-x}\text{In}_x$  near  $x=0$  can be explained by the  $\text{LaSn}_3$  Fermi surface possessing small pockets of electrons which disappear as one alloys with In at  $x \approx 1$ .

Our measurements of  $S_x(T)$  indicate that Ce in  $\text{LaIn}_3$  (but not in  $\text{LaSn}_3$ ) is a Kondo system, while  $\rho(H)$  vs  $T$  for  $\text{LaIn}_3$  and  $\text{LaSn}_3$ , and  $R_H(T)$  for  $\text{LaIn}_3$  indicate that the number of holes or electrons in these compounds is not temperature dependent. We have also inferred a structural phase trans-